

DOE/MC/22044-15  
Distribution Category UC-122

**IMPROVED CO<sub>2</sub> ENHANCED OIL RECOVERY -- MOBILITY  
CONTROL BY IN-SITU CHEMICAL PRECIPITATION**

**Final Report**

By

Samuel Ameri  
Khashayar Aminian  
James A. Wasson  
David L. Durham

**DOE/MC/22044--15**

**DE91 002243**

**June 1991**

**Work Performed Under Contract No. DE-AC21-85MC22044**

Prepared for  
U.S. Department of Energy  
Assistant Secretary for Fossil Energy

Royal J. Watts, Project Manager  
Morgantown Energy Technology Center  
P. O. Box 880  
Morgantown, WV 26505

Prepared by  
West Virginia University  
Department of Petroleum and Natural Gas Engineering  
Morgantown, WV 26505

**MASTER**

DISTRIBUTION OF THIS DOCUMENT IS UNLIMITED

## ABSTRACT

CO<sub>2</sub> Flooding is the most promising enhanced oil recovery method. However, the highly mobile CO<sub>2</sub> seeks out the path of least resistance through the largest pore openings and takes the most direct route between the injection well and the production well. This causes early breakthrough and reduces CO<sub>2</sub> sweep efficiency. As a result, CO<sub>2</sub> flooding is often not economically feasible without better CO<sub>2</sub> mobility control. Several methods of mobility control have been attempted with limited success. Therefore, new concepts for controlling the mobility of injected CO<sub>2</sub> are required to improve the overall sweep efficiency and economics.

To overcome the tendency of CO<sub>2</sub> to bypass the smaller pores containing the residual oil, one approach would be to plug the larger pores by chemical precipitation. Several relatively inexpensive water soluble salts of earth alkali group react with CO<sub>2</sub> to form precipitate. Once the precipitate is formed in the larger pores, the subsequent fluid flow will be diverted to relatively smaller pores, thereby increasing the sweep efficiency.

The overall objective of this study has been to evaluate the feasibility of chemical precipitation to improve CO<sub>2</sub> sweep efficiency and mobility control. The laboratory experiments have indicated that carbonate precipitation can alter the permeability of the core samples under reservoir conditions. Furthermore, the relative permeability measurements have revealed that precipitation reduces the gas permeability in favor of liquid permeability. This indicates that precipitation is occurring preferentially in the larger pores. Additional experimental work with a series of connected cores have indicated that the permeability profile can be successfully modified. However, pH control plays a critical role in propagation of the chemical precipitation reaction. A numerical reservoir model has been utilized to evaluate the effects of permeability heterogeneity and permeability modification on the CO<sub>2</sub> sweep efficiency.

The computer simulation results indicate that the permeability profile modification can significantly enhance CO<sub>2</sub> vertical and horizontal sweep efficiencies. The scoping studies with the model have further revealed that only a fraction of high permeability zones need to be altered to achieve sweep efficiency enhancement.

## TABLE OF CONTENTS

	PAGE
ABSTRACT	iii
TABLE OF CONTENTS	v
LIST OF TABLES	viii
LIST OF FIGURES	ix

### CHAPTER ONE - INTRODUCTION

1.1	Background	1
1.2	The Proposed CO <sub>2</sub> Sweep Improvement Method	2
1.3	Research Objectives	3
1.4	Project Organization	5
1.5	Publications	7

### CHAPTER TWO - REVIEW OF CURRENT TECHNOLOGY

1	Background	9
2.2	Sweep Improvement Methods	13
2.3	Reservoir Modification Methods	17
2.4	Carbonate Precipitation	18
2.5	Summary and Conclusions	19
2.6	References	19

**TABLE OF CONTENTS (continued)**

	Page
<b>CHAPTER THREE - CARBONATE PRECIPITATION TESTS</b>	
3.1	Introduction
3.2	Ambient Tests
3.3	Chemistry of Reaction
3.4	Buffer Solution Tests
3.5	Carbonate Precipitation Under Reservoir Conditions
3.6	Summary and Conclusions
3.7	References
<b>CHAPTER FOUR - CARBONATE PRECIPITATION IN THE CORE SAMPLES</b>	
4.1	Sand Pack Test
4.2	Core Tests
4.3	Multiple Core Tests
4.4	Relative Permeability Tests
4.5	Multiple Slug - Multiple Core Test
4.6	Oil Saturated Core Tests
4.7	Discussion
4.8	Summary and Conclusions
4.9	References

**TABLE OF CONTENTS (continued)**

	<b>Page</b>
<b>CHAPTER FIVE - SIMULATION STUDIES</b>	
5.1      Introduction	102
5.2      Description of Reservoir Model	103
5.3      Simulation Studies	105
5.4      Summary and Conclusions	114
5.5      References	118
 <b>NOMENCLATURE</b>	
	<b>119</b>

## **LIST OF TABLES**

	<b>PAGE</b>
3.1 CaCl <sub>2</sub> Ambient Test Results	29
3.2 BaCl <sub>2</sub> Ambient Test Results	30
3.3 Ambient Slug Test Results	33
3.4 Borax and CaCl <sub>2</sub> Ambient Test Results	37
3.5 Borax and BaCl <sub>2</sub> Ambient Test Results	38
3.6 CaCl <sub>2</sub> Reservoir Conditions Test Results	46
3.7 BaCl <sub>2</sub> Reservoir Conditions Test Results	48
3.8 Precipitation Test Results in Long Window Cell	51
4.1 Sand Pack Test Information	57
4.2 The Effect of CO <sub>2</sub> Saturation on Core Sample Permeability	59
4.3 Core Test Results Utilizing Buffer Solution at 1500 psig and 100°F	61
4.4 Single Core Test Results at 1500 psig and 100°F	73
4.5 Single Core Test Results at 2000 psig and 100°F	74
4.6 Aging Core Test Results at 1500 psig and 100°F	76
4.7 Multiple Core Test Results at 1500 psig and 100°F	80
4.8 Permeability Reduction During the Multiple Slug Experiment in 3 Connected Cores at 1500 psig and 100°F	97

## *LIST OF FIGURES*

	<b>PAGE</b>
1.1 CO <sub>2</sub> Flow Path in a Depleted Oil Reservoir	4
1.2 Carbonate Precipitation Modifies the Permeability Profile	4
1.3 CO <sub>2</sub> Flow Path after Carbonate Precipitation	4
3.1 The Effect of Ph on Carbonate Precipitation	36
3.2 Schematic of Experimental Set-up for Reservoir Conditions Tests	45
4.1 The Schematic Diagram of the Core Holder	64
4.2 The Schematic Diagram of the Experimental Set-up for Single Core Tests	65
4.3 The Schematic Diagram of the Experimental Set-up for Multiple Core Tests	79
4.4 The Schematic Diagram of Gas-Water Relative Permeability Apparatus	90
4.5 The Comparison of Measured Relative Permeability Ratio's with the Published Data	90
4.6 The Effect of Calcium Carbonate Precipitation at 1500 psig and 100°F on the Relative Permeability of Berea Core Sample	92
4.7 The Effect of Calcium Carbonate Precipitation at 2000 psig and 100°F on the Relative Permeability of Berea Core Sample	92
4.8 The Effect of Barium Carbonate Precipitation at 1500 psig and 100°F on the Relative Permeability of Berea Core Sample	93
4.9 The Effect of Barium Carbonate Precipitation at 2000 psig and 100°F on the Relative Permeability of Berea Core Sample	93

***LIST OF FIGURES (continued)***

	<b>PAGE</b>
4.10 The Effect of Carbonate Precipitation at 1500 psig and 100°F on Gas Relative Permeability in Multi-Slug Tests	96
4.11 The Effect of Barium Carbonate Precipitation on 3rd Core in the Multi-Slug Tests	96
5.1 The Reservoir Model Used for Immiscible CO <sub>2</sub> Flooding Simulations	107
5.2 The Effect of Precipitation on Oil Recovery Efficiency for Immiscible CO <sub>2</sub> Flooding	107
5.3 The Reservoir Model Used for Horizontal Sweep Efficiency Simulations	110
5.4 The Effect of Horizontal Heterogeneity on Oil Sweep Efficiency by Miscible CO <sub>2</sub> Flooding	111
5.5 The Effect of Precipitation Propagation on the Oil Horizontal Sweep Efficiency by Miscible CO <sub>2</sub> Flooding	111
5.6 The Effect of Horizontal Heterogeneity on Oil Production Rates During Miscible CO <sub>2</sub> Flooding	112
5.7 The Effect of Precipitation Propagation on Oil Production Rates During Miscible CO <sub>2</sub> Flooding	112
5.8 The Effect of Percent of Permeability Reduction by Precipitation on Oil Sweep Efficiency	113
5.9 The Effect of Percent of Permeability Reduction by Precipitation on Oil Production Rates	113

*LIST OF FIGURES (continued)*

	PAGE
5.10 The Reservoir Model Used for Vertical Sweep Efficiency Simulations	115
5.11 The Effect of Vertical Heterogeneity on Oil Sweep Efficiency by Miscible CO <sub>2</sub> Flooding	116
5.12 The Effect of Precipitation Propagation on the Oil Vertical Sweep Efficiency by Miscible CO <sub>2</sub> Flooding	116
5.13 The Effect of Vertical Heterogeneity on Oil Production Rates During Miscible CO <sub>2</sub> Flooding	117
5.14 The Effect of Precipitation Propagation on Oil Production Rates During Miscible CO <sub>2</sub> Flooding	117

## CHAPTER ONE

### **1.1. Background**

CO<sub>2</sub> flooding is one of the most promising and fastest growing enhanced oil recovery method. A major problem in enhanced oil recovery (EOR) in general and CO<sub>2</sub> flooding in particular is low volumetric sweep efficiency. Reservoir heterogeneities are widely recognized as some of the major contributors to low volumetric sweep efficiency often encountered in enhanced oil recovery processes. The unfavorable permeability contrasts within the reservoir result in channeling of injected fluids through high permeability streaks. When channeling occurs, oil in tighter parts of a reservoir is bypassed. To recover the uncontacted or unswept oil, it is necessary to redirect the injected CO<sub>2</sub> from well-swept regions of the reservoir to low permeability regions that are poorly swept and usually contain significant amounts of oil.

Techniques for recovering oil from the uncontacted or unswept areas are referred to as sweep improvements methods and include both mobility control and reservoir modification techniques. The purpose of any sweep improvement method is to prevent cycling of injected fluids through high permeability layers of the reservoir. Several methods for CO<sub>2</sub> sweep improvement have been proposed with limited success. Therefore, new concepts for enhancing CO<sub>2</sub> sweep efficiency are required to improve

recovery and economics. The overall objective of this research program is to provide an improved technology base for increasing ultimate oil recovery from  $\text{CO}_2$  miscible and immiscible EOR operations while maintaining project economics that allow the implementation of the improved technology. The efforts in this research program more specifically are directed at  $\text{CO}_2$  sweep improvement by in-situ carbonate precipitation.

## **1.2. The Proposed $\text{CO}_2$ Sweep improvement Method**

A treatment that could reduce the permeability of the high permeability regions throughout the reservoir would effectively reduce the channeling, divert the flow of the displacing fluid through the less permeable regions, improve the sweep efficiency, and increase oil recovery. The petroleum engineering literature contains numerous references to formation damage (permeability reduction) due to carbonate precipitation (scale). This indicates that if proper conditions exist in the porous media, the controlled formation of carbonate precipitates would cause permeability reduction.

One procedure used in  $\text{CO}_2$  flooding, known as WAG, is conducted by injecting a slug of water and following it with a  $\text{CO}_2$  slug.  $\text{CO}_2$  flows most readily through the most permeable regions and bypasses the residual oil in less permeable regions as illustrated in Figure 1.1 for a hypothetical heterogeneous porous media. Several relatively inexpensive water soluble salts of the earth alkali group react with  $\text{CO}_2$  to form a solid carbonate precipitate. If the water slug contains a solution of one of the above

mentioned salts, the carbonate precipitate will be formed in the regions that are contacted by the subsequent CO<sub>2</sub> slug. As a result, the majority of the precipitate will be formed in the high permeability channels that are swept by CO<sub>2</sub>. Formation of the precipitate will result in partial plugging of the large pores in the high permeability region, thereby reducing their permeability as illustrated in Figure 1.2. Once the precipitation has reduced the permeability in the high permeability regions, subsequent CO<sub>2</sub> slugs will be forced to flow through an alternate path as shown in Figure 1.3. Each WAG cycle will repeat the process with additional precipitate forming in progressively lower permeability zones. The salt in the injected water can be discontinued any time the permeability modification is no longer desired.

### **1.3. Research Objectives**

The overall goal of this research program has been to develop an improved technology base for increasing ultimate oil recovery from CO<sub>2</sub> miscible and/or immiscible EOR operations while improving the economics over the current state-of-the-art practices to allow the implementation of improved technology. More specifically, the research efforts are directed at evaluating the feasibility of utilizing in situ carbonate precipitation for CO<sub>2</sub> sweep improvement.

The specific objectives of the research program are:

- To determine and evaluate the optimum conditions and materials for chemical

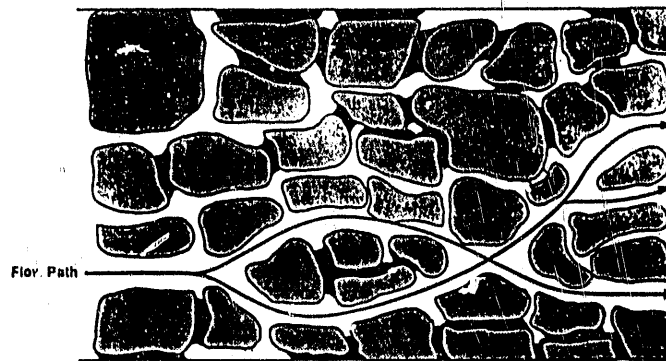


Fig. 1.1.  $\text{CO}_2$  Flow Path in a Depleted Oil Reservoir

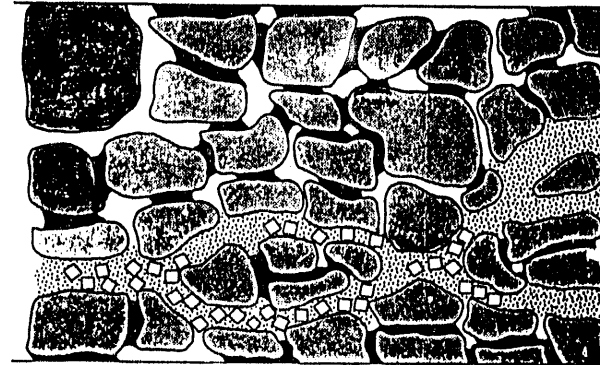


Fig. 1.2. Carbonate Precipitation Modifies the Permeability Profile



Fig. 1.3.  $\text{CO}_2$  Flow Path After Carbonate Precipitation

precipitation over a realistic range of reservoir pressures and temperatures.

- To evaluate the permeability alteration by in situ chemical precipitation in core samples.
- To extend the laboratory results by modeling and computer simulation to determine the expected increased oil recovery through the application of the in-situ precipitation.

#### **1.4. Project Organization**

The research efforts in this project are divided into 4 phases or tasks as described below.

##### **1.4.1. Task I - Review of Current Technology**

A complete review of the literature pertaining to volumetric sweep efficiency enhancement and mobility control was conducted prior to the start of the laboratory research. This review determined the necessity for research in the area of sweep efficiency enhancement. The results of the literature reviews are summarized in Chapter 2.

#### **1.4.2. Task II - Carbonate Precipitation Experiments**

The efforts in this task were directed at determining the conditions and materials for optimum in-situ precipitation over a realistic range of reservoir pressures and temperatures. The first step of this task involved the selection of chemicals that are readily water soluble, inexpensive, and that form a solid precipitate when contacted by CO<sub>2</sub>. These experiments were conducted at ambient conditions. The second step of this task involved the carbonate precipitation experiments that were carried out under reservoir conditions in a PVT cell. The experimental procedures as well as the results of the experiments are provided in Chapter 3.

#### **1.4.3. Task III - Carbonate Precipitation in Core Samples**

The experiments in this task involved the attempts to modify the permeability by in-situ carbonate precipitation in the core samples. Several series of tests under a variety of conditions were conducted in Berea core samples 1 1/2 inches in diameter and 6 inches long in order to evaluate the permeability alteration. The experimental procedures as well as the results of the experiments are provided in Chapter 4.

#### **1.4.4. Task IV - Modeling and Computer Simulation**

A reservoir model was utilized in this phase of the research to extend the experimental results to field applications and to determine the enhancement in the

horizontal and vertical sweep efficiencies due to carbonate precipitation. The results of the computer simulations are provided and discussed in Chapter 5.

### **1.5. Publications**

The following publications, theses, and presentations have resulted from this research project.

1. P.S. Puon, S. Ameri, K. Aminian, D.L. Durham, J.A. Wasson, and R.J. Watts: "CO<sub>2</sub> Mobility Control by Carbonate Precipitation: Experimental Study", SPE 18529, Proceedings of SPE Eastern Regional Conference, Charleston, WV, Nov. 1988.
2. K. Aminian, S. Ameri, and R.J. Watts: "CO<sub>2</sub> Mobility Control by Carbonate Precipitation - A Feasibility Study", Paper 98H, Presented at AIChE Annual Conference, Enhanced Oil Recovery Perspective III, Washington, D.C., Dec. 1988.
3. K. Aminian, L.E. Cunningham, S. Ameri, and R.J. Watts: "Carbonate Precipitation to Improve CO<sub>2</sub> Mobility Control", Presented at Eastern Regional American Chemical Society Conference, Cleveland, OH, June 1989.
4. K. Aminian, S. Ameri, L.E. Cunningham, and R.J. Watts: "CO<sub>2</sub> Mobility Control by

Carbonate Precipitation: A Modeling Study", SPE 19321, Proceedings of SPE Eastern Regional Conference, Morgantown, WV, Nov. 1989.

5. K. Aminian, S. Ameri, and R.J. Watts: "A Modeling Study of CO<sub>2</sub> Sweep Efficiency Enhancement by Carbonate Precipitation", Paper 59B, Presented at AIChE Spring National Meeting, Enhanced Oil Recovery II, Orlando, FL, March 1990.
6. R.M. Burger: "A Preliminary Study of CO<sub>2</sub> Mobility Control by In-Situ Chemical Precipitation", Master's Thesis, West Virginia University, Petroleum and Natural Gas Engineering Department, May 1988.
7. D.K. Gosnell: "CO<sub>2</sub> Mobility Control by In-Situ Chemical Precipitation - A Core Study", Master's Thesis, West Virginia University, Petroleum and Natural Gas Engineering Department, Dec. 1988.
8. D. Nay: "Evaluation of Permeability Profile Modification During Carbonate Precipitation in Core Samples", Master's Thesis, West Virginia University, Petroleum and Natural Gas Engineering Department, Under Preparation.
9. L.E. Cunningham: "CO<sub>2</sub> Mobility Control by In-Situ Chemical Precipitation Computer Modeling Study", Master's Thesis, West Virginia University, Petroleum and Natural Gas Engineering Department, Under Preparation.

## CHAPTER TWO

### **REVIEW OF CURRENT TECHNOLOGY**

A complete review of the literature pertaining to sweep efficiency enhancement and mobility control was conducted prior to the start of the laboratory research. Although this literature search was specifically directed at CO<sub>2</sub> sweep improvements, attention was also focused on work done to improve sweep efficiency in conventional, secondary, and other enhanced oil recovery procedures.

Standard and prevalent procedures including formal literature search, computerized literature and patent search, and communication with the professional community was used to locate and document the related material. A continuing effort was made throughout the project to keep the review current and complete. This review determined and proved the necessity for research in the area of sweep improvements. This chapter summarizes the results of the literature search and provides the background on CO<sub>2</sub> flooding and sweep improvement methods.

#### **2.1. Background**

Oil recovery by CO<sub>2</sub> flooding has been extensively discussed in the literature<sup>(1-5)</sup>. This section provides only a brief review of this topic.

After secondary recovery of oil by waterflooding, a certain amount of residual oil remains in the pore spaces of the reservoir rock for one or both of two reasons: (1) the

oil was bypassed and not contacted by the injected water; or (2) capillary forces retained the oil in the pore spaces. The retention of oil in the reservoir pore spaces is caused by interfacial effects between two immiscible fluids. The importance of the role that capillary and interfacial forces play in controlling fluid movement and the efficiency of the recovery mechanism have long been recognized. Carbon Dioxide (CO<sub>2</sub>) has the potential to overcome both of these factors. Many crude oils are miscible with CO<sub>2</sub> under certain conditions of temperature and pressure. Miscibility eliminates the interface between fluids and reduces the capillary retaining forces to essentially zero.

There is a difference between CO<sub>2</sub> dissolving in crude oil and CO<sub>2</sub> being miscible with crude oil. As pressure is applied to a CO<sub>2</sub>-crude oil system, the CO<sub>2</sub> will readily dissolve until the crude oil is saturated with CO<sub>2</sub> at the existing pressure and temperature. At that time, there will be both free CO<sub>2</sub> and CO<sub>2</sub>-saturated crude oil present with an interface between the two fluids. Dissolving the CO<sub>2</sub> in this manner will result in an expansion of the CO<sub>2</sub>-crude oil solution and a reduction of its viscosity. Solution of the CO<sub>2</sub> in this manner will take place regardless of the composition or API gravity of the crude oil. It is obvious that the swelling of the oil will increase the oil saturation in the reservoir rock and will, therefore, enhance the relative permeability of the reservoir rock to oil. In addition, the residual oil saturation that remains after recovery operations are complete will consist of swollen oil, which consists of a large volume of CO<sub>2</sub> and a relatively small quantity of hydrocarbon material. The reduction of viscosity and the

increase in relative permeability to oil, both facilitate flow of the swollen oil to the production well. Thus, immiscible displacement, a result of dissolving CO<sub>2</sub> in crude oil, may frequently be an effective enhanced oil recovery technique.

The processes described above also take place in miscible CO<sub>2</sub> displacement. Miscibility between CO<sub>2</sub> and crude oil, however, requires more restrictive conditions of temperature, pressure, and oil composition than simply the dissolving of CO<sub>2</sub> in the oil. Miscibility entails, by definition, the elimination of the interface between the CO<sub>2</sub> and the oil. At any given temperature and for any given crude oil, there is a minimum miscibility pressure (usually 1000 psi or greater), MMP, below which the interface will remain. In most cases, CO<sub>2</sub> and crude oil, because of differences in their properties and composition, will not be miscible on first contact, regardless of pressure. These fluids have what is called multiple contact miscibility. In other words, the CO<sub>2</sub> must repeatedly contact the oil and, because of the concentration gradient between the oil and the CO<sub>2</sub>, many hydrocarbon molecules, especially those of C<sub>5</sub>-C<sub>30</sub>, must leave the oil and enter the CO<sub>2</sub>. After a sufficient number of contacts, enough of these hydrocarbons will have joined the CO<sub>2</sub>-rich phase and enough CO<sub>2</sub> will have entered the hydrocarbon-rich phase so that the two phases become miscible. At that time, the interface between the phases will disappear, capillary forces will become zero, and the residual oil saturation can be reduced to less than 10 percent of the pore space in the contacted portions of the reservoir.

In order to determine the chances of conducting a successful miscible CO<sub>2</sub> displacement, information must be obtained from several sources. Slim tube tests - in which tubing smaller than 0.25 inch I.D., and at least 80 feet long, are packed with glass beads or unconsolidated sand, and saturated with reservoir oil, is flooded with CO<sub>2</sub> at reservoir temperature and various pressures - in order to determine the Minimum Miscibility Pressure (MMP). In these tests, multiple contact miscibility can be attained at MMP or pressures greater than MMP.

Core samples of reservoir rock saturated with reservoir oil and formation water are flooded with CO<sub>2</sub> at a temperature and pressure greater than MMP in order to determine, in a more realistic situation, the residual oil saturation (S<sub>o</sub>) and the permeability effects that may be expected in a field application. Wettability of the core samples should be preserved and determined as an aid in predicting the amount of oil that may be trapped by water blocking.

Additional reservoir data, such as the permeability profile, the vertical-permeability to horizontal-permeability ratio, and transmissibility between reservoir strata are needed for reservoir studies.

A permeability profile having widely varying permeabilities in a reservoir formation with a natural or induced fracture system that is poorly oriented with respect to the well pattern, would indicate that this reservoir is a poor candidate for CO<sub>2</sub> flooding or most other EOR techniques. Because of the low density of CO<sub>2</sub> gas compared to that of oil,

there is a tendency for the CO<sub>2</sub> to migrate vertically to the top of the formation (gravity override), i.e., to advance more rapidly at the top of the reservoir than in lower portions of the rock. The low viscosity of CO<sub>2</sub> gas permits the formation of viscous fingers or small channels in which the CO<sub>2</sub> rapidly moves from the injection well to the production well, bypassing a large part of the oil saturated reservoir.

The viscosity factor and the abnormally high relative permeability to gases at low gas saturations result in a very high mobility for the CO<sub>2</sub>. This mobility, in turn, because of the channeling and fingering that it produces and the absence of oil banking that it permits, results in a generally low volumetric sweep efficiency, rapidly increasing the producing CO<sub>2</sub>-oil ratios, and necessitating the recovery and reinjection of large volumes of produced CO<sub>2</sub>.

## **2.2. Sweep Improvement Methods**

As discussed in the previous section, additional oil recovery from an already water-flooded reservoir can be achieved by CO<sub>2</sub> injection. However, the recovery efficiency, as with any fluid driven process, depends on the degree of bypass or channeling. The injected CO<sub>2</sub> has a strong tendency to flow through those pores that have been contacted and largely saturated with the displacing water. Reservoir heterogeneities, such as fractures, channels, or high-permeability streaks, can cause CO<sub>2</sub> channeling and thus result in poor sweep efficiency, early CO<sub>2</sub> breakthrough, and

reduced oil recovery. To recover the uncontacted or unswept oil, it is, therefore, necessary to direct the injected  $\text{CO}_2$  into the previously unswept portions of the reservoir. Techniques for recovering oil from the uncontacted or unswept areas are referred to as sweep improvement methods and include both mobility control and reservoir modification techniques. The purpose of any sweep improvement method is to prevent cycling of the injected fluid ( $\text{CO}_2$ ) through high-permeability layers of the reservoir.

Sweep improvement is, therefore, important for successful  $\text{CO}_2$  flooding. Several methods have been proposed in attempts to alleviate the situation, but none of them have been successful to a satisfactory degree. The point of entry of the  $\text{CO}_2$  into the reservoir can be controlled by seating one or more packers at an appropriate position(s) or by selective perforation of the casing. However, once the  $\text{CO}_2$  leaves the immediate vicinity of the wellbore, this method cannot control its movement. Production wells can be shut in or flow can be restricted. Without the pressure sink which they normally provide, there will be less tendency for the  $\text{CO}_2$  to channel until they are put on production once more.

### **2.2.1. Water Alternating Gas (WAG)**

The earliest attempt to reduce  $\text{CO}_2$  mobility was with a water alternating gas (WAG) process. In this process, a slug of gas ( $\text{CO}_2$ ) is injected and then is followed by a slug of water. The water injection tends to reduce the relative permeability to gas and

thus decreases  $\text{CO}_2$  mobility<sup>(6)</sup>. Although this method may temporarily reduce the channeling tendency of the  $\text{CO}_2$ , relative permeability to water and  $\text{CO}_2$  remains high in the already formed channels. Also, any increase in conformance may be lost because of the lower displacement efficiency that occurs here as a result of water preceding the  $\text{CO}_2$  through the pore spaces. This problem is worse in the case of previously watered out reservoirs. Stalkup has reviewed results of several  $\text{CO}_2$  floods and concluded that the WAG was only "partially successful in moderating  $\text{CO}_2$  production"<sup>(7)</sup>.

### 2.2.2. Foams

Attempts have been made to improve the WAG process sweep efficiency by adding surfactants to the injected water<sup>(8,9)</sup>. The use of foams to reduce  $\text{CO}_2$  mobility was initially presented by Bernard and Holm<sup>(10)</sup> and has been the subject of a number of publications since that time<sup>(11,12,13)</sup>. In this method, water with a foaming agent (surfactant) is injected into the formation followed by  $\text{CO}_2$ . When  $\text{CO}_2$  contacts the surfactant-water solution, foam or emulsion is formed. The foam impedes the formation of  $\text{CO}_2$  viscous fingering and also gives a better sweep efficiency.

Patton et.al.<sup>(9)</sup> have studied the different foaming agents that might be employed in  $\text{CO}_2$  flooding. They found that anionic surfactants performed well in static foam tests. In the dynamic foam test, ethoxylated alcohol (a nonionic surfactant) lowered the gas mobility by a factor of 2 over that of the Alipal CD-128/Monomid 150-AD (an anionic

Survey", DOE/MC/10698-3, Oct. 1980.

15. Casteel, J.F., and Djabbarah, N.F.: "Sweep Improvements in Carbon Dioxide Flooding Using Foaming Agents", SPE 14392, presented at Ann. SPE Tech. Conf., Sept. 1985.
16. Heller, J.P., Boone, D.A., and Watts, R.F.: "Field Tests of CO<sub>2</sub> Mobility Control at Rock Creek", SPE 14395, presented at Ann. SPE Tech. Conf., Sept. 1985.
17. Heller, J.P., D.K. Dange, R.J. Card, and L.G. Donaruma: "Direct Thickeners for Mobility Control of CO<sub>2</sub> Floods", Soc. Pet. Eng. Jour., Oct. 1985.
18. Berston, J.N.: "Selective Plugging of Waterflood Input Wells Theory, Methods, and Results", Jour. of Pet. Tech., May 1957.
19. Garland, T.M.: "Selective Plugging of Water Injection Wells", Jour. of Pet. Tech., Dec. 1966.
20. Richardson, E.A.: "Plugging a Subterranean Formation by Homogeneous Solution Precipitate", Patent No. 3,614,985, Filed March 30, 1970, Ser. No. 23,550, Int. Cl. E21b 33/138, U.S. Cl. 166-294.
21. Richardson, E.A. and Scheuerman, R.F.: "Plugging Solution Precipitation Time Control", Patent No. 3,730,272, Filed May 17, 1971, Ser. No. 144,260, Int. Cl. E21b 33/13,43/25 U.S. Cl. 166-294.
22. Sarem, A.M.: "Mobility-Controlled Caustic Flood", Patent No. 3,805,893, Filed Aug. 28, 1972, Ser. No. 284,345, Int. Cl. E21b 43/22, U.S. Cl. 166-270.

23. Clampitt, R.L. and Hesserl, J.E.: "Method for Controlling Formation Permeability", Patent No. 3,785,437, Filed Oct. 4, 1972, Ser. No. 294,990, Int. Cl. E21b 33/138,43/27, U.S. Cl. 166-281.
24. Felber, B.J. and Dauben, D.L.: "Laboratory Development of Lignosulfonate Gels for Sweep Improvements", SPE 6206, presented at 51st SPE Ann. Tech. Conf., New Orleans, LA, Oct. 1976.
25. Hess, P.H.: "One-Step Furyfuryl Alcohol Process for Formation Plugging", Jour. Pet. Tech., 1980.
26. Borchhardt, J.K.: "Method of Reducing the Permeability of a Subterranean Formation", to Halliburton Co., Duncan, OK, U.S. Patent 4,600,057, Filed April 1, 1985.
27. Dalryple, D. and Vinson, E.: "Method of Altering the Permeability of a Hydrocarbon-Containing Subterranean Formation", to Halliburton Co., Duncan, OK, U.S. Patent 4,617,132, Filed April 1, 1985.
28. Shu, P.: "Programmed Gelation of Polymers for Oil Reservoir Permeability Control", to Mobil Oil, New York, NY, U.S. Patent 40,606,407, Filed Nov. 29, 1984.
29. Wagner, O.R., Weisrock, W.P., and Patel, C.: "Field Application of Lignosulfonate Gels to Reduce Channeling, South Swan Miscible Unit, Alberta, Canada", presented at the 61st SPE Ann. Tech. Conf., New Orleans, LA, Oct.

1986.

30. Martin, F.D. and Kovarick, F.S.: "Chemical Gels for Diverting CO<sub>2</sub> - Baseline Experiments", SPE 16728, presentd at the 62nd SPE Ann. Tech. Conf., Dallas, TX, Sept. 1987.
31. Parmenswar, R. and G.P. Willhite: "A Study of the Reduction of Brine Permeability in Berea Sandstone Using Aluminum Citrate Process", SPE 13582, Proc. of SPE Oil Field and Geothermal Chemistry, April 9-11, 1985.
32. Willhite, G.P., Green, D.W., Thiele, J.L., Young, T., and Meters, K.B.: "Investigation of the Application of Gelled Polymers Systems for Permeability Modification in Petroleum Reservoirs", Final Report, DOE Contract, DOE/BC/10843-15, March 1990.
33. Torrest, R.S. and Haung, S.H.: "Alumina Precipitation in Porous Media for Profile Control", SPE 16251, Proc. of SPE Oil Field and Geothermal Chemistry, Feb. 1987.
34. Oddo, J.E., Sloan, K.M., and Mason, B.: "Inhibition of CaCO<sub>3</sub> Precipitation from Brine Solutions - A New Flow System for High-Temperature and High-Pressure Studies", Jour. Pet. Tech., Oct. 1982.
35. Tomson, M.B., Rogers, L.A., Varughese, K., Preswich, S.M., and Salimi, M.H.: "Use of Inhibitors for Scale Control in Brine-Producing Gas and Oil Wells", SPE 15457, presented at the 61st SPE Ann. Tech. Conf., New Orleans, LA, Oct. 1986.

36. Hausler, R.H.: "Predicting and Controlling Scale from Oil-Field Brines", Oil and Gas Journal, Sept. 18, 1978.
37. Underdown, D.R. and Newhouse, D.P.: "Evaluation of Calcium Carbonate Scale Inhibitors for Prudhoe Bay Alaska", SPE 15658, presented at the 61st SPE Ann. Tech. Conf., New Orleans, LA, Oct. 1986.
38. Shaughnessy, C.M. and Kline, W.E.: "EDTA Removes Formation Damage at Prudhoe Bay", SPE 11188, presented at the 57th SPE Ann. Tech. Conf., New Orleans, LA, Oct. 1982.
39. Rogers, L.A., Tomson, M.B., Matty, J.M., and Durrett, L.R.: "Saturation Index Predicts Brine's Scale-Forming Tendency", Oil and Gas Journal, April 1, 1985.
40. Oddo, J.E. and Tomson, M.B.: "Simplified Calculation of  $\text{CaCO}_3$  Saturation at High Temperatures and Pressures", Jour. pet. Tech., July 1982.
41. Street, E.V. and Oddo, J.E.: "Scale Control Aids Gas Recovery", Jour. Pet. Tech., Oct. 1989.
42. Nancollas, G.H. and Sawada, K.: "Formation of Scale of Calcium Carbonate Polymorphs - The Influence of Magnesium Ion and Inhibitors", Jour. Pet. Tech., March 1982.
43. Krumrine, P.H., Mayer, E.H., and Brock, G.F.: "Scale Formation During Alkaline Flooding", Jour. Pet. Tech., Aug. 1985.
44. Ramsey, J.E. and Cenegy, L.M.: "A Laboratory Evaluation of Barium Sulfate

Scale Inhibitors at Low Ph for Use in Carbon Dioxide EOR Floods", SPE 14407, presented at the 60th Ann. Tech. Conf., Las Vegas, NV, Sept. 1985.

45. Patton, J.T., P.F. Phelan, G. Smith, and J.D. Chavez: "CO<sub>2</sub> Formation Damage Study", Final Report, Contract DOE/MC/10865-13, July 1983.

## CHAPTER THREE

### CARBONATE PRECIPITATION TESTS

#### **3.1. Introduction**

The efforts in this task were directed at selecting the chemicals and determining the conditions for optimum in situ precipitation. The objective was achieved by combining various chemicals with CO<sub>2</sub> to form precipitate under pressures and temperatures similar to those encountered in the reservoirs. These high pressure and temperature tests were conducted in a PVT cell available in the Petroleum Engineering PVT Laboratory at West Virginia University.

#### **3.2. Ambient Tests**

To reduce the number of tests necessary to be performed in the PVT cell, a series of tests at ambient conditions were performed in order to select the suitable chemicals and their concentrations.

##### **3.2.1. Chemical Selection**

The ambient phase of the tests began by selecting chemicals that were water soluble, inexpensive, and that formed a solid precipitate when contacted by CO<sub>2</sub>. Based on preliminary literature review MgO, CaO, CaCl<sub>2</sub>, MgCl<sub>2</sub>, and BaCl<sub>2</sub> were considered as potential candidates. However, after some preliminary tests, MgO and CaO were

eliminated from consideration because of their limited solubility. Furthermore,  $MgCl_2$  was eliminated as a potential candidate because of the high solubility of  $MgCO_3$ . Therefore,  $CaCl_2$  and  $BaCl_2$  were utilized throughout the remainder of these experiments.

### **3.2.2. Ambient Precipitation Tests**

A series of experiments were conducted to study how the salt, the salt concentration, and Ph of the solution affect the volume of precipitate. The procedure used during these tests is outlined below:

1. 300 ml samples of salt solutions were prepared, each at concentrations of 0.1%, 1%, and 2.5%.
2.  $CO_2$  was bubbled through the salt solutions for a period of 15 minutes.
3. The Ph of the solution was adjusted to the desired test Ph (6, 7, 8, 9, and 10) by adding NaOH.
4. The precipitate was then filtered out of the solution and dried and weighed.

Tables 3.1 and 3.2 contain the results of the precipitation tests under ambient conditions. The higher concentrations of salts, as can be seen in both tables, do not appear to yield a higher percentage of precipitate. It is reasonable to conclude that the amount of  $CO_2$  dissolved in the solution is the limiting factor. By comparing the results in the two tables, it is evident that the percentage of  $BaCO_3$ ,

precipitate is higher than that of the  $\text{CaCO}_3$  precipitate. This is due to the smaller precipitation constant for  $\text{BaCO}_3$ .

### **3.2.3. Ambient Slug Tests**

One concern relative to the effectiveness of the precipitate was, that lowering of the Ph when  $\text{CO}_2$  was reintroduced into solution would dissolve the precipitate already formed. Consequently, a series of slug tests were run under ambient conditions. Two separate types of slug tests were run; one alternated only  $\text{CO}_2$  and  $\text{NaOH}$  while the other alternated salt,  $\text{CO}_2$ , and  $\text{NaOH}$ . The Slug Test procedure was as follows:

1. 300 ml of salt solution was prepared and the Ph was recorded.
- 2a. Series I: 300 ml of salt solution was dispensed into a beaker.
- 2b. Series II: 100 ml of salt solution was dispensed into a beaker.
3.  $\text{CO}_2$  was bubbled at 10 psig through the salt solution for 15 minutes.
4. Ph was recorded.
5.  $\text{NaOH}$  was added to adjust the Ph to the desired test Ph.
6. The precipitate was filtered, dried, and weighed.
7. The percentage of material collected was then calculated.

Series I slug tests were conducted by alternating  $\text{CO}_2$  and  $\text{NaOH}$  in a given amount of salt solution. The one cycle slug test was performed following the previously listed procedure. The two cycle slug tests were performed by repeating steps 3 through

**TABLE 3.1. CaCl<sub>2</sub> Ambient Test Results**

<u>Test Ph</u>	<u>CaCl<sub>2</sub> Conc.</u>	<u>Weight of Precipitate (gms)</u>	<u>% of Ca<sup>++</sup> collected</u>
6	.1%	0	-
7	.1%	0	-
8	.1%	0	-
9	.1%	.24	82%
10	.1%	.31	100%
6	1.0%	0	-
7	1.0%	0	-
8	1.0%	1.23	46%
9	1.0%	1.24	46%
10	1.0%	1.26	47%
6	2.5%	0	-
7	2.5%	1.24	20%
8	2.5%	1.24	20%
9	2.5%	1.25	20%
10	2.5%	1.42	20%

**TABLE 3.2. BaCl<sub>2</sub> Ambient Test Results**

<u>Test Ph</u>	<u>CaCl<sub>2</sub> Conc.</u>	<u>Weight of Precipitate (gms)</u>	<u>% of Ca<sup>++</sup> collected</u>
7	.1%	.20	70%
8	.1%	.32	100%
9	.1%	.32	100%
10	.1%	.33	100%
6	1.0%	0	-
7	1.0%	2.07	73%
8	1.0%	2.08	74%
9	1.0%	2.53	89%
10	1.0%	2.53	89%
6	2.5%	.60	9%
7	2.5%	1.90	27%
8	2.5%	2.34	33%
9	2.5%	2.45	35%
10	2.5%	2.41	34%

5 once before implementing steps 6 and 7. The three cycle slug tests were conducted by repeating steps 3 through 5 twice before implementing steps 6 and 7. The percentage of material collected was calculated and used to establish whether the precipitate had dissolved or if more precipitate had been formed by the slugs.

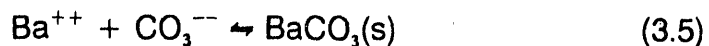
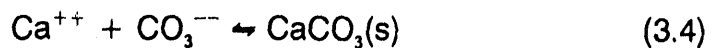
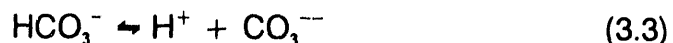
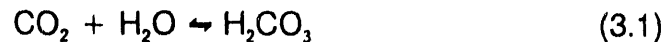
The Series II slug tests were completed by alternating slugs of the salt solution, CO<sub>2</sub>, and NaOH. In the one cycle slug test, the previously listed procedure was followed. The two cycle slug tests were conducted by repeating steps 2 through 5 once before implement steps 6 and 7. The three cycle test was performed by repeating steps 2 through 5 twice prior to steps 6 and 7. The percentage of material collected was calculated and used to determine if the precipitate was dissolved by the subsequent CO<sub>2</sub> injection.

The results from the ambient slug tests are given in Table 3.3. The best results were achieved in the three cycle tests for all cases. This was expected after observing the original ambient tests. Since the CO<sub>2</sub> dissolved in these original tests did not use all of the salt ion available, it was believed that if more CO<sub>2</sub> could be dissolved, more precipitate would form. These tests also indicate that additional slugs of CO<sub>2</sub> do not redissolve the precipitate. As seen in Table 3.3, the best results were obtained from the three cycle, Series I tests. This would indicate that the best injection scheme would be to inject a large slug of the salt solution and then alternate slugs of CO<sub>2</sub> and NaOH. It also appears from the data that the best chemical in these slug tests was BaCl<sub>2</sub>. This is

seen in the last column of Table 3.3 where the percentage of Barium collected was greater than the percentage of Calcium collected under similar conditions. One problem associated with barium may be the small particle size of the precipitate. As in the original ambient tests, some of the precipitate passed through the filter paper when filtering.

### 3.3. Chemistry of the Reaction

In the experiments for this work,  $\text{CO}_2$  was mixed with a salt solution, either  $\text{CaCl}_2$  or  $\text{BaCl}_2$ . The  $\text{CO}_2$  combined with the water in the salt solution to form carbonic acid. This dissociated to form the anion  $\text{HCO}_3^-$  (bicarbonate) and, eventually,  $\text{CO}_3^{--}$  (carbonate) formed. The  $\text{CO}_3^{--}$  anion combined with the cation of the salt to form either  $\text{CaCO}_3$  or  $\text{BaCO}_3$  as the Ph increased. The chemical equations for this reaction are shown below:



The carbonate precipitate, although present under any pressure and temperature, is more prevalent under high pressures, temperatures, and Ph. As the temperature and Ph increase, the solubility of the carbonate decreases, thereby allowing it to precipitate. This

**TABLE 3.3 Ambient Slug Test Results**

**2.5% BaCl<sub>2</sub>**

**Series I**

	NaOH (cc)	NaOH (cc)	NaOH (cc)	Ph	NaOH (gm)	ppt (gm)	Ba <sup>++</sup> (gm)	Ba <sup>++</sup> available % collected
A	40.5	-	-	7.0	1.85	1.287	4.940	26.1
B	44	55.9	-	7.0	4.43	3.081	4.940	62.4
C	46	51.5	42.5	7.0	6.63	4.611	4.940	93.3

**Series II**

	NaOH (cc)	NaOH (cc)	NaOH (cc)	Ph	NaOH (gm)	ppt (gm)	Ba <sup>++</sup> (gm)	Ba <sup>++</sup> available % collected
A	14	-	-	7.0	0.63	0.438	1.647	26.6
B	15.3	38	-	7.0	2.42	1.683	3.293	51.1
C	14.9	39	54.5	7.0	5.25	3.651	4.940	73.9

**2.5% CaCl<sub>2</sub>**

**Series I**

	NaOH (cc)	NaOH (cc)	NaOH (cc)	Ph	NaOH (gm)	ppt (gm)	Ca <sup>++</sup> (gm)	Ca <sup>++</sup> available % collected
A	44	-	-	9.0	1.09	0.436	2.730	16.1
B	44	58	-	9.0	2.59	1.036	2.730	38.3
C	45	67	78	9.0	4.79	1.916	2.730	70.9

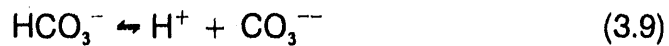
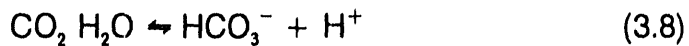
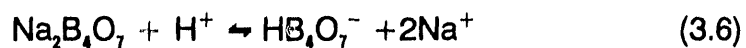
**Series II**

	NaOH (cc)	NaOH (cc)	NaOH (cc)	Ph	NaOH (gm)	ppt (gm)	Ca <sup>++</sup> (gm)	Ca <sup>++</sup> available % collected
A	14.5	-	-	10.0	0.39	0.156	0.901	17.3
B	17.5	39.5	-	10.0	1.20	0.48	1.802	26.6
C	15.6	43.1	74.3	10.0	2.11	1.244	2.730	46.0

fact is illustrated in Figure 3.1<sup>(1)</sup>. This is evident by the fact that the enthalpy change reaction of dissolving  $\text{CaCO}_3$  is negative. Raising the temperature tends to drive the equilibrium of the reaction described here to the precipitation side of the reaction. The higher the Ph, the greater the amount of precipitation obtained.

### 3.4. Buffer Solution Tests

Two concerns that were raised during the precipitation tests were the control of the Ph and the mixing of the chemical in the porous media. A buffer solution (Borax) was considered<sup>(2)</sup> to be mixed with the salt prior to injection, so that the chemicals could be premixed to ensure complete mixing, and to achieve the highest Ph. The chemistry of the Borax,  $\text{CO}_2$ ,  $\text{NaOH}$ , and  $\text{CaCl}_2$  reaction is:



The above reaction would be the same if  $\text{BaCl}_2$  was used.

Numerous ambient tests were performed using varying concentrations and amounts of buffer, salt, and sodium hydroxide. Tables 3.4 and 3.5 summarize the results

of the ambient tests. These ambient tests showed promising results.

### **3.5. Carbonate Precipitation Under Reservoir Conditions**

This phase of the research dealt with carbonate precipitation under pressures and temperatures comparable to those encountered in a reservoir. It should be noted that although it was possible to produce precipitate under ambient conditions, it was necessary to determine the optimum conditions for precipitation under reservoir pressure and temperature conditions.

#### **3.5.1. Theoretical Approach**

Prior to experimental research, it was attempted to search and establish the theoretical models in the area of carbonate precipitation at high pressures and temperatures.

A computer program entitled "SOLGASMIX-PV" was located and obtained<sup>(3,4)</sup>. The program has been designed to calculate precipitate formation based on the chemical content, temperature and pressure of the sample. However, this program made no provisions for aqueous solutions and could not be applied to this research. After further investigation, a computer model designed to calculate chemical precipitation in aqueous solutions was located<sup>(5,6,7)</sup>. A copy of the program entitled "SOLGASWATER" was purchased and was placed into the WVNET System. The program was reviewed and

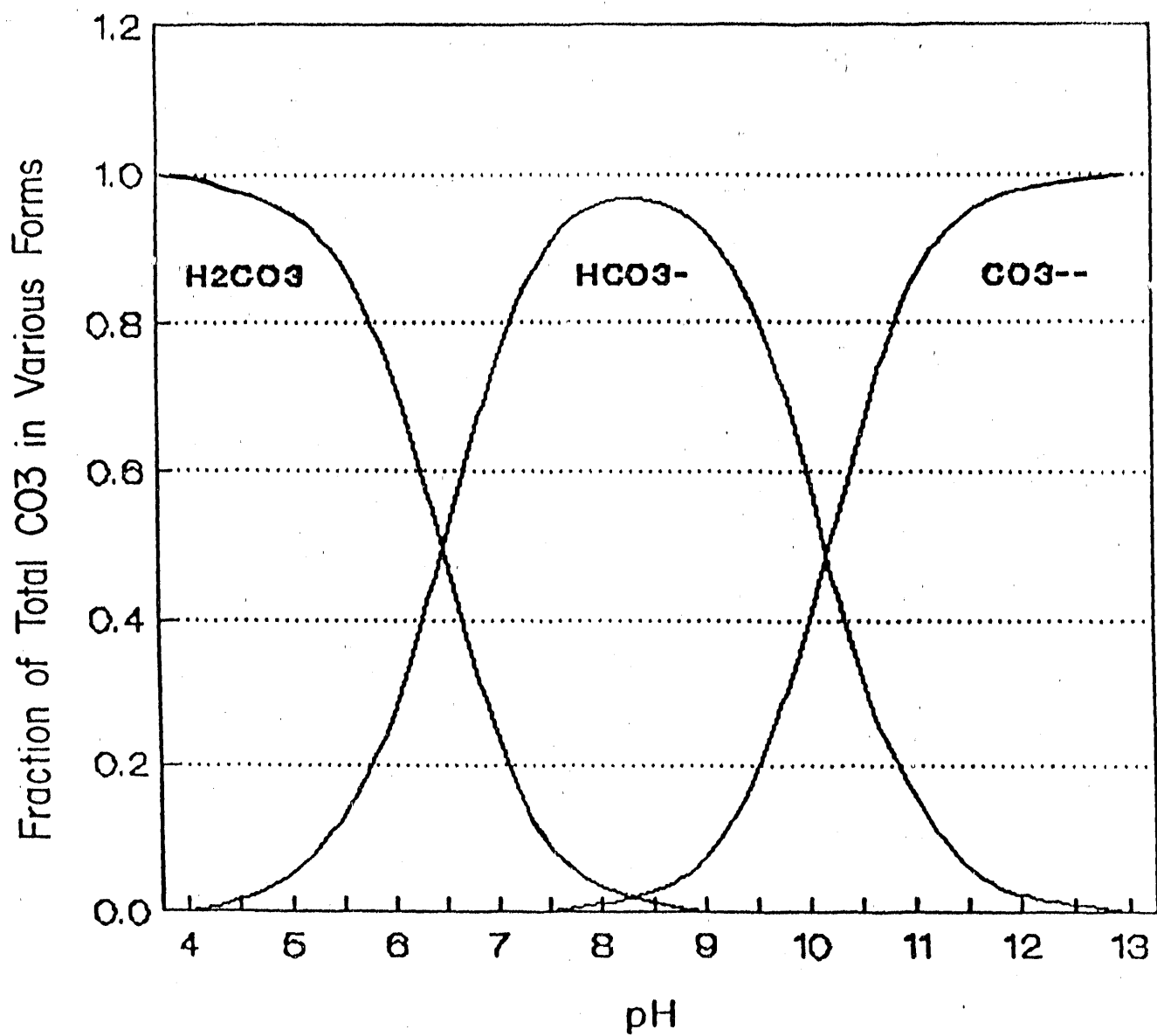


Fig. 3.1. The Effect of pH on Carbonate Precipitation

**TABLE 3.4 Borax and CaCl<sub>2</sub> Ambient Test Results**

No.	Conc. Borax (M)	Amt. (ml)	Conc. CaCl <sub>2</sub> (M)	Arnt. (ml)	CO <sub>2</sub> time (sec)	Ph	Precip wt (g)
1a	0.084	6	0.30	25	5	10.8	0.13
1	0.084	10	0.25	40	6	10.6	0.18
2	0.084	10	0.20	40	3	10.9	0.22
3	0.084	10	0.15	40	3	11.1	0.19
4	0.084	10	0.10	40	3	11.1	0.14
5	0.084	10	0.05	40	3	11.4	0.10
6	0.067	10	0.25	40	4	10.8	0.16
7	0.067	10	0.20	40	4	11.0	0.12
8	0.067	10	0.15	40	4	11.1	0.14
9	0.067	10	0.10	40	4	11.1	0.11
10	0.067	10	0.05	40	5	11.4	0.10
11a	0.050	12	0.30	25	2	11.1	0.15
11	0.050	20	0.25	40	5	11.0	0.18
12	0.050	20	0.20	40	5	11.1	0.32
13	0.050	20	0.15	40	5	11.1	0.19
14	0.050	20	0.10	40	4	11.4	0.22
15	0.050	20	0.05	40	4	11.4	0.06

Note: Tests 1-10 6 ml of 0.25M NaOH was added raising the Ph approximately 1.5 (8.4 - 10.9)

Note: Tests 11-15 9 ml of 0.25M NaOH was added raising the Ph approximately 1.5 (8.6 - 11.1)

Note: Test 1a 4 ml of 0.25M NaOH was added raising the Ph approximately 1.8 (9.2 - 11.0)

Note: Test 11a 6 ml of 0.25M NaOH was added raising the Ph approximately 2.5 (8.7 - 11.2)

TABLE 3.5 Borax and BaCl<sub>2</sub>, Ambient Test Results

No.	Conc. Borax (M)	Amt. (ml)	Conc. CaCl <sub>2</sub> (M)	Amt. (ml)	CO <sub>2</sub> time (sec)	Ph	Precip wt (g)
1	0.084	7	0.25	40	18	8.4	0.08
2	0.084	7	0.20	40	17	8.2	0.08
3	0.084	7	0.15	40	25	8.1	0.09
4	0.084	7	0.10	40	33	8.0	0.09
5	0.084	7	0.05	40	17	8.4	0.08
6	0.067	12	0.25	40	70	7.7	0.09
7	0.067	12	0.20	40	32	7.6	0.135
8	0.067	12	0.15	40	35	7.3	0.11
9	0.067	12	0.10	40	37	7.4	0.10
10	0.067	12	0.05	40	36	7.5	0.08
11	0.050	15	0.25	40	29	7.3	0.13
12	0.050	15	0.20	40	28	7.4	0.12
13	0.050	15	0.15	40	33	7.3	0.14
14	0.050	15	0.10	40	34	7.4	0.10
15	0.050	15	0.05	40	38	7.8	0.09
16	0.034	45	0.25	40	71	7.5	0.26
17	0.034	45	0.20	40	66	7.1	0.24
18	0.034	45	0.15	40	60	7.3	0.25
19	0.034	45	0.10	40	77	7.4	0.21
20	0.084	7	0.25	40	12	8.7	0.16
21	0.084	7	0.20	40	15	8.5	0.17
22	0.084	7	0.15	40	13	8.6	0.18
23	0.084	7	0.10	40	9	8.9	0.17
24	0.084	7	0.05	40	24	8.8	0.18
25	0.034	45	0.25	40	17	8.9	0.49
26	0.034	45	0.20	40	10	9.1	0.57
27	0.034	45	0.15	40	11	9.0	0.44
28	0.034	45	0.10	40	12	9.2	0.43

Notes on following page

Note: Tests 20-24 2 ml of 0.25M NaOH was added raising the Ph approximately 0.5

Note: Tests 25-28 5 ml of 0.25M NaOH was added raising the Ph approximately 0.5 Note: No additional precipitate was noted when additional CO<sub>2</sub> was bubbled through the effluent of tests 20-28.

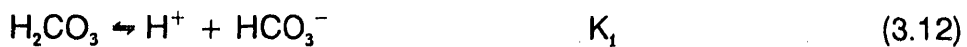
In all tests the maximum amount of NaOH was added without forming OH<sup>-</sup> precipitate.

problems were encountered in linking the model. The linking problem was due primarily to the lack of the necessary sub-routines in the system.

### 3.5.2. Carbonate Model

It was attempted to develop a model for carbonate precipitation after the existing model was found to be unusable for this research work.

The carbonate system in a geological environment has been investigated quite extensively<sup>(8,9)</sup>. A carbonate system that exists in a reservoir will have several thermodynamic equilibrium equations satisfied. These thermodynamic equilibrium equations relate the activities or concentrations of each of the species concerned. Equations involved in the equilibrium are the dissociation equilibrium of carbonate, bicarbonate, and water; the solubility product of the carbonate precipitate involved; and the partial pressure of CO<sub>2</sub> and carbonic acid. All the equations involved will be expressed in mathematical formula as the following:



Activities, rather than concentrations, will be used in the thermodynamic

equilibrium. All the ionic species under reservoir conditions contribute to the activity coefficients of  $\text{Ca}^{++}$ ,  $\text{HCO}_3^-$ ,  $\text{CO}_3^{--}$ , and  $\text{OH}^-$ . It is common to use the Debye-Hückel equation to evaluate the activity coefficients as a function of ionic strength. The concentrations of all the pertinent species will be found after equations (3.12) - (3.16) have been solved simultaneously. In order to have a carbonate precipitate to occur, the product of

$$\gamma M_i^{++} \gamma \text{CO}_3^{--} [M^{++}][\text{CO}_3^{--}]$$

needs to exceed its  $K_{sp}$  value, otherwise the ionic species will remain in the aqueous phase. The model states that under atmospheric pressure, for a 0.001 M concentration of  $\text{Ca}^{++}$ ,  $\text{CaCO}_3$  will precipitate above Ph 9. For  $\text{Ba}^{++}$ , that has a slightly lower solubility product than  $\text{CaCO}_3$ , the Ph value required for  $\text{BaCO}_3$  to precipitate is similar.

When carbon dioxide pressure increases, more  $\text{CO}_2$  dissolves in the aqueous phase, thus more  $\text{H}_2\text{CO}_3$  will be in the aqueous phase. A higher concentration of  $\text{H}_2\text{CO}_3$  will shift the equilibrium to the right, and a higher concentration of  $\text{CO}_3^{--}$  will result. The solubility product is a constant; therefore, a higher concentration of  $\text{CO}_3^{--}$  will indicate that a lower concentration of  $\text{Ca}^{++}$  or  $\text{Ba}^{++}$  is tolerable in the solution and eventually the required Ph value to precipitate the carbonate salt is decreased. For instance, at 14.7 psia of  $\text{CO}_2$ , the Ph required for  $\text{CaCO}_3$ , and  $\text{BaCO}_3$  to precipitate are 7 and 6, respectively. For a much higher pressure of  $\text{CO}_2$ , such as 1200 psia, still lower pH's may be required to precipitate their carbonate salt.

There is no need to overemphasize that the mathematical model and, subsequently, its calculation results are based on the following assumptions:

1. closed system, under thermodynamic equilibrium
2. ionic strength for the solution is 0.1
3. common ion interference does not exist
4. thermodynamic constants are known at given temperatures and pressures

Condition 1 has to be satisfied for any models involved with equilibrium studies and it is no exception for this model. For condition 2, the 0.1 ionic strength is chosen for its close resemblance to the actual connate water concentrations. In the actual implementation of this model a water analysis may be required. The third assumption merely states that only a single  $M^{++}$  species exists in the system. If referring to a field case, it means the concentration of  $M^{++}$  naturally occurring is negligible compared with the injection concentration of  $M^{++}$  (not necessarily the same with the first one).

Thermodynamic constants used in this model are at ambient temperature and pressure. However, an earlier study has shown that at temperatures and pressures other than ambient, the variants of these values are limited. When adapting this model to a real reservoir, a safety factor may be allowed to compensate for the differences.

When applying this model to an actual field or even a core flooding, it is important to realize that some of the conditions may not apply. We especially need to know that, unlike a closed system, thermodynamic equilibrium may not occur in a reservoir or in a

core flood test. It is best to apply this model with a safety factor that ensures the proper results will be obtained. It is recommended that an additional 1 to 2 pH units be allowed when evaluating the final calculation results. Nevertheless, this model study provides a way to understand the relations existing between all the parameters involved in a reservoir under equilibrium conditions.

### **3.5.3. Experimental Evaluations**

The experimental phase of the research involved the same chemical reactions as the ambient tests; however, the experiments were carried out under reservoir temperature and pressure conditions in the PVT cell. This was achieved by combining the chemical solutions with CO<sub>2</sub> under various pressures and temperatures to form the precipitate. The two chemicals which produced the best results under ambient conditions, CaCl<sub>2</sub> and BaCl<sub>2</sub>, were chosen for the PVT tests.

These tests were performed using a PVT (Pressure, Volume, Temperature) cell using mercury as the compressing agent for pressure adjustment. Pressure was monitored by a mercury pump pressure gauge, while the temperature was monitored using a thermometer inserted in the PVT cell. Figure 3.2 is the schematic of the apparatus used in reservoir condition tests. The procedures for these experiments are shown below:

1. Approximately 200 ml of air was evacuated from the cell with a vacuum pump.

2. 100 cc of salt solution was drawn into the cell and the remaining 100 cc of space was re-evacuated using a vacuum pump.
3. The CO<sub>2</sub> supply was attached to the cell and 33 cc of liquid CO<sub>2</sub> was injected into the cell.
4. The cell was raised to the desired pressure and temperature for the test, and agitated for 5 minutes to thoroughly mix the CO<sub>2</sub> and salt solution while the pressure and temperature were closely monitored.
5. A second mercury pump was charged with the desired amount of NaOH needed for the test and was brought to test pressure.
6. The NaOH was transferred to the cell at the test pressure.
7. The cell was agitated for 15 minutes, with the test pressure and temperature closely monitored.
8. The mixture was visually inspected through the cell window to verify that precipitation had occurred.
9. The pressure was released and the mixture was quickly removed from the cell.
10. The final pH of the mixture was measured and then the mixture was filtered.
11. The precipitate was dried and weighed and the weight was recorded.

The first chemical used under pressure and temperature conditions was CaCl<sub>2</sub>.

The results from these tests are shown in Table 3.6. The first three tests were performed to study the effect of pressure on precipitation at a given temperature. From the results

of these three tests, it was established that 0.5M NaOH did not raise the pH to the desired level. The final pH of the solution was below 7 and the percentage of the Calcium precipitate collected remained at 33% for all pressures. Next, the amount of NaOH added to the mixture was doubled to increase the pH. This increased the amount of precipitate collected. The increase in the volume of NaOH seemed impractical; subsequently, it was attempted to increase pH by increasing the molar concentration of NaOH. The next two tests examined the effect of temperature on precipitation. As can be seen from Table 3.6, temperature did not appear to have a significant effect. Increasing the molar concentration of NaOH did increase pH but did not increase the amount of precipitate collected. The effect of temperature on precipitation was again examined at a higher concentration of NaOH. Again, temperature showed little effect. The next four tests used successively increasing concentrations of NaOH to attempt to increase the amount of precipitate. As can be seen from Table 3.6, as NaOH concentration increased, precipitation increased. This was expected due to the increase in pH with higher NaOH concentrations. The final three tests were performed to examine the effect of pressure on precipitation. The 1M NaOH and 1.0%  $\text{CaCl}_2$  concentration were chosen for comparison purposes. The amount of precipitate increased slightly with increasing pressure.

The other salt used in PVT testing was  $\text{BaCl}_2$ . The results of these tests are shown in Table 3.7. The first three tests on  $\text{BaCl}_2$  examine the effect of pressure on precipitation.

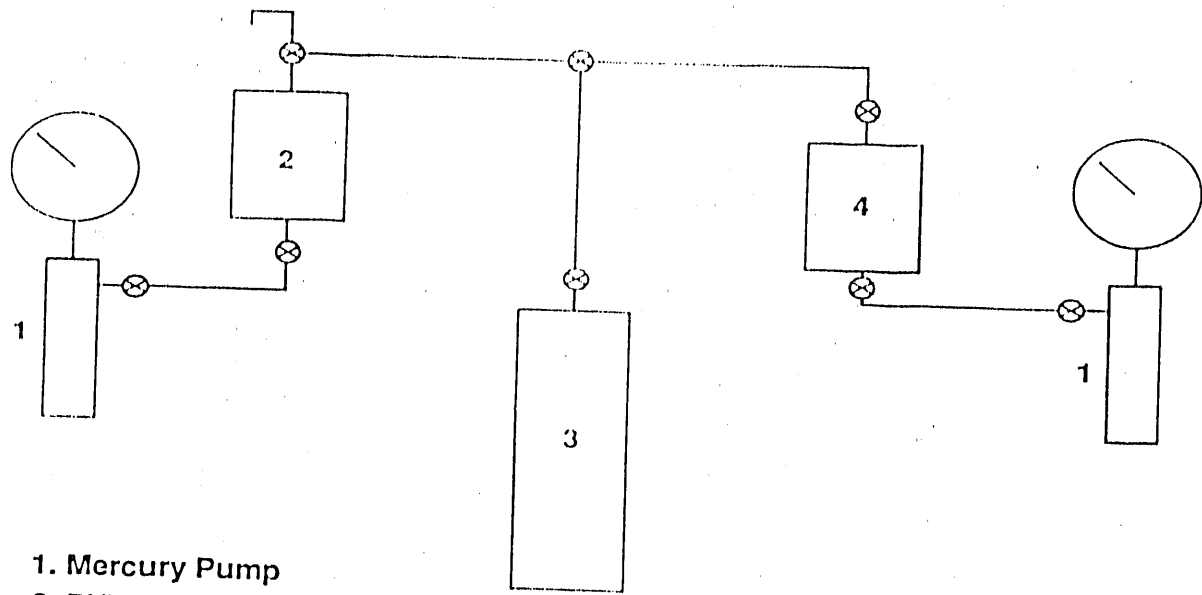


Fig. 3.2. Schematic of Experimental Set-up for Reservoir Conditions Precipitation Tests.

TABLE 3.6 CaCl<sub>2</sub> Reservoir Conditions Test Results

<u>Test No.</u>	<u>CaCl<sub>2</sub> Conc.</u>	<u>NaOH added</u>	<u>Press. (psi)</u>	<u>Temp. (°F)</u>	<u>Final pH</u>	<u>% of Ca<sup>++</sup> collected</u>
1(1)	1%	.5M	1500	100	6.45	33%
2(2)	1%	.5M	2000	100	6.48	33%
3(3)	1%	.5M	2500	100	6.47	33%
4(7)	1%	.5M	1500	100	6.68	75%
5(5)	1%	.5M	1500	100	6.65	22%
6(6)	1%	.5M	1500	100	6.50	31%
7(9)	1%	1M	1500	100	6.85	22%
8(8)	1%	1M	2000	100	7.01	22%
9(12)	1%	1M	1500	100	6.77	19%
10(13)	1%	1M	1500	100	7.30	17%
11(14)	1%	2M	1500	100	7.44	36%
12(15)	1%	3M	1500	100	7.75	56%
13(16)	1%	4M	1500	100	7.71	92%
14(17)	1%	4M	1500	100	7.75	100%
15(11)	2.5%	1M	1500	100	6.64	13%
16(4)	2.5%	1M	2000	100	6.45	16%
17(10)	2.5%	1M	2000	100	6.49	16%

There appears to be an optimum pressure for precipitation formation of approximately 1500 psia. As shown in Table 3.7, the amount of precipitate collected at 1500 psig was significantly higher than at 1000 psig or 2000 psig. It also appears that as pressure increases above 1500 psia, precipitation decreases. This was supported from the fact that the amount of precipitate at 2000 psig was even lower than the amount at 1000 psig. The next three tests examined how an increased NaOH concentration would affect precipitation. As illustrated in Table 3.7, this did have a beneficial effect on the amount of precipitate. In this case, as pressure increased the amount of precipitate increased. The next three tests were performed using a 2.5% BaCl<sub>2</sub> concentration and examining the effect of pressure. As in the first 1.0% BaCl<sub>2</sub> tests, there seemed to be an optimum pressure at 1500 psig. As in the 1.0% BaCl<sub>2</sub> tests, the effect of temperature was the amount of precipitate. In this case, as pressure increased the amount of precipitate increased. The next three tests were performed using a 2.5% BaCl<sub>2</sub> concentration and examining the effect of pressure. As in the first 1.0% BaCl<sub>2</sub> tests, there seemed to be an optimum pressure at 1500 psig. As in the 1.0% BaCl<sub>2</sub> tests, the effect of temperature was examined. As temperature increased, precipitated increased. This was opposite of the 1.0% BaCl<sub>2</sub> tests 7 and 8 in Table 3.7 and also did not agree with the CaCl<sub>2</sub> tests 9 and 10 in Table 3.6. These tests are very qualitative since the test solution is lowered to ambient conditions prior to collecting and weighing the precipitate.

TABLE 3.7 BaCl<sub>2</sub> Reservoir Conditions Test Results

<u>Test No.</u>	<u>BaCl<sub>2</sub> Conc.</u>	<u>NaOH added</u>	<u>Press. (psi)</u>	<u>Temp. (°F)</u>	<u>Final pH</u>	<u>% of Ba<sup>++</sup> collected</u>
1(31)	1%	.5M	1000	100	6.59	80%
2(20)	1%	.5M	1500	100	6.65	94%
3(21)	1%	.5M	2000	100	6.87	30%
4(25)	1%	1M	1000	100	6.43	95%
5(32)	1%	1M	1500	100	6.54	100%
6(23)	1%	1M	2000	100	7.05	100%*
7(26)	1%	1M	1500	75	6.46	83%
8(27)	1%	1M	2000	100	6.82	67%
9(19)	2.5%	1M	1000	100	6.78	90%
10(21)	2.5%	1M	1500	100	6.06	100%
11(24)	2.5%	1M	2000	100	6.21	69%
12(29)	2.5%	1M	1500	75	6.01	74%
13(28)	2.5%	1M	1500	100	6.19	90%
14(30)	2.5%	3M	1500	100	7.50	100%*

\*pH above 7.0 apparently causes one of the other chemicals to precipitate out thus yielding a weight of Ba<sup>++</sup> artificially higher than possible. It is assumed that all the Ba<sup>++</sup> (100%) was collected.

### **3.5.4. Long Window Cell Experiments**

According to Tomson, et.al., carbonates will precipitate out as pressure is reduced. Therefore, the weight of the precipitate collected in PVT cell tests can only be used qualitatively. For this reason, it was decided to attempt to obtain more quantitative results using a long window PVT cell, where the amount of precipitate could be measured at test conditions. These tests will be discussed later.

The procedure using the long window PVT cell was basically the same as for the previously described PVT cell test. The chemicals were added in the same sequence and in the same amounts. The only difference was that after two hours of mixing the materials together, the height of the precipitate in the window was measured. This measurement is still qualitative because there is no way of knowing how much liquid is left in the precipitate. The pressure may also compress the precipitate making it appear that there is less precipitate formed at higher pressures. There may also be a problem if the height measurements are taken at different times, because the precipitate settles slightly when left under pressure for longer time periods, thus reducing the height. One advantage of the long window cell over the regular PVT cell is that pH indicators added to the solution could be viewed in order to obtain some general information about the pH under test conditions.

As can be seen in Table 3.8, both 2.5%  $\text{CaCl}_2$  and 2.5%  $\text{BaCl}_2$  were used in the long window cell. The first two tests, both with  $\text{CaCl}_2$ , indicated the importance of pH.

As shown, the precipitate level was higher at a pH greater than 8 than at a pH less than 8. The first two tests with BaCl<sub>2</sub> also indicated the importance of pH. The final two tests in Table 3.8 indicate temperature could have some effect on the precipitation. As shown, more precipitate forms at lower temperatures. This contradicts the results of the PVT cell. In the PVT cell tests, however, the precipitate was not measured under pressure and temperature. In fact, the lower temperature should have more precipitate because more CO<sub>2</sub> can dissolve in the solution. This trend will continue until the temperature is low enough to allow liquid CO<sub>2</sub> to be present. At this point, there is less CO<sub>2</sub> in solution, thus reducing the amount of precipitate formed.

### **3.6. Summary and Conclusions**

The theoretical and experimental evaluations indicate the carbonate precipitate can be formed under pressure and temperature conditions that are encountered in the reservoir. It appears a pressure range of 1500-2000 psia, a temperature of 100° F, and 2.5% concentration of salt, are the optimum conditions for precipitation. It should, however, be noted that pH plays a significant role on the amount of precipitate formed. The higher the pH, the more precipitate will form. However, achieving high pH values may not be realistic in the reservoir<sup>(10)</sup>. The minimum required pH appears to be about 8.

TABLE 3.8 Precipitation Test Results in Long Window Cell

<u>No.</u>	<u>Chemical</u>	<u>Test Conditions</u>	<u>Ht. (in.) of Precip. (2 hours time)</u>	<u>pH</u>
1	CaCl <sub>2</sub>	1500 psig 120° F	0.985	>8
2	CaCl <sub>2</sub>	1500 psig 120° F	0.945	<8
3	BaCl <sub>2</sub>	1500 psig 150° F	1.650	≤ 8.5
4	BaCl <sub>2</sub>	1500 psig 120° F	0.690	<7
5	BaCl <sub>2</sub>	2000 psig 150° F	0.565	8
4	BaCl <sub>2</sub>	2000 psig 120° F	0.810	8

### 3.7. References

1. Blaedel, W.J. and Melodre, V.W.: Elementary Quantitative Analysis, Theory and Practices, 2nd. Edition, McGraw Hill, 1982.
2. Stien, W.: Personal Communication, Rehoboth Beach, Delaware, 1988.
3. Besmann, T.M.: "SOLGASMIX-PV, A Computer Program to Calculate Equilibrium Relationships in Complex Chemical System", Oakridge National Laboratory, Contract No. W-7405-eng-26, ORNL/TM-5775, 1977.
4. Carling, R.W. and Mar, R.W.: "Application of complex Equilibrium Calculations to the Study of Mineral Matter During coal Combustion", Sandia Report, SAND82-8035, Feb. 1983.
5. Ericksson, G.: "Thermodynamic Studies of High Temperature Equilibria", ACTA, Chemica Scandinavica, 25, 1971.
6. Erickson, G.: "Tehrmodynamic Studies of High Temperature Equilibria III", Chemica Scripta, 1973.
7. Erickson, G.: "Thermodynamic Studies of High Temperature Equilibria, IV", Chemica Scripta, 1975.
8. Garrels, R.M. and Christ, C.L.: Solution, Minerals and Equilibria, Freemen, Cooper & Company, 1965.

9. Lowenthal, R.E. and Marais, G.V.R.: "Carbonate Chemistry of Aquatic Systems: Theory and Application", Ann Arbor Science Publisher, Inc., 1976.
10. Ramakrishnan, T.S. and Wassan, D.T.: "The Role of Adsorption in High pH Flooding", SPE Paper 17408, Presented at SPE California Regional Meeting, March 1988.

## CHAPTER FOUR

### CARBONATE PRECIPITATION IN THE CORE SAMPLE

The purpose of this task was to investigate the precipitation formation under flowing (dynamic) conditions in the porous media in order to evaluate the feasibility of carbonate precipitation as a mobility control for CO<sub>2</sub> flooding. To gain a better understanding of the carbonate precipitation process in the porous media and achieve the research objectives, carbonate precipitation tests were conducted in Berea core samples.

The precipitate causes reduction in core permeability. As a result, the measurement of core sample permeability before and after the precipitation can be used to verify the formation of precipitate under reservoir conditions. In addition, several other aspects of precipitation in the cores were of interest. They included:

- (a) The percentage of reduction in the core permeability due to carbonate precipitation.
- (b) The effect of precipitation on the permeability profile.
- (c) Mixing of chemicals in the cores.
- (d) The depth of precipitation propagation in the core samples.

As a result, two series of tests were designed and conducted in the core samples. The first series of tests utilized a single core while the second series of tests utilized 2 or 3 connected cores. The complete description of the test procedures and the results are

provided in the following sections.

#### **4.1. Sand Pack Test**

A preliminary sand pack test was performed prior to precipitation tests in the core samples. The purpose of the sand pack test was to verify that precipitation can occur under dynamic conditions at reservoir pressure. The pertinent information on the sand pack tests are provided in Table 4.1. The procedure for this test is summarized below:

1. Sand was packed in a long pipe.
2. The sand pack permeability to brine was measured.
3. 2 pore volumes (PV) of  $\text{BaCl}_2$  were pumped through the sand pack under ambient conditions to displace the brine.
4. The sand pack was pressurized to the test pressure with  $\text{BaCl}_2$ .
5. 2 more PV of  $\text{BaCl}_2$  were pumped through sand pack under pressure.
6. Approximately 1 PV of  $\text{CO}_2$  was pumped into the sand pack.
7. 2 PV of  $\text{NaOH}$  were pumped through the sand pack to raise the pH.
8. 2 PV of brine were pumped through the apparatus to displace all unreacted chemicals.
9. The pressure was reduced to the ambient conditions.
10. The permeability to brine was measured.
11. The percentage of reduction in permeability was then calculated.

The sand pack permeability was reduced from 206 Darcies to 109 Darcies or 47%. It was, therefore, concluded that carbonate precipitation had occurred under flowing conditions in the porous media.

#### **4.2. Core Tests**

The purpose of the core tests was to study and evaluate carbonate precipitation in porous media under flowing conditions. The procedures and conditions of the experiments and chemicals were selected based on the optimum conditions determined through previous experimental investigations. The core samples utilized during the experiments consisted of Berea sandstone core samples 6-inch long and 1-1/2 inch in diameter. The chemicals used in the core tests were 0.25 molar (M)  $\text{BaCl}_2$  and  $\text{CaCl}_2$ . 1.0 M  $\text{NaOH}$  was used to adjust the pH.

The formation of carbonate precipitation in the core samples will cause permeability reduction, as was observed in the sand pack test. Therefore, a reduction in permeability of the core sample after the test will verify the formation of precipitate under dynamic conditions in the cores.

##### **4.2.1. Blank Test**

The permeability of the cores decreased from the deposition of precipitate. The reduction, however, could also have been caused by the reaction between the chemicals

TABLE 4.1 Sand Pack Test Information

Test Conditions:

- $P = 1500$  psig
- $T = 120^{\circ}\text{F}$
- Salt = 2.5%  $\text{BaCl}_2$
- $\text{NaOH} = 1\text{M}$

Dimensions:

- $L = 5.5$  ft.
- $D = 3/4$  inch
- Sand Size = 20/40 Mesh
- Permeability = 206 Darcies

and the core sample. To assure that the permeability reduction after the test is caused only by precipitation, a blank test was conducted. The blank test was performed by injecting the individual materials (i.e.  $\text{CaCl}_2$ ,  $\text{CO}_2$ , and  $\text{NaOH}$ ) into the core sample separately followed by brine to flush the injected material out of the core. Afterwards, the core permeability was measured and was compared to the original core permeability. These tests indicated that the core permeability is significantly reduced after  $\text{CO}_2$  injection. The results of the permeability reduction due to  $\text{CO}_2$  flooding are summarized in Table 4.2. The reduction in permeability is caused by residual gas ( $\text{CO}_2$ ) saturation formed in the core. Therefore, it is important to account for the permeability reduction due to residual gas saturation. As a result, the cores were first flooded with  $\text{CO}_2$  and the permeability reduction due to residual  $\text{CO}_2$  saturation was determined. Subsequently, the cores were subjected to carbonate precipitation test and the final core permeability was determined. The comparison of the final permeability and permeability with residual gas saturation can verify the formation of precipitate in the core. A pre-test  $\text{CO}_2$  flooding procedure was developed and will be discussed in the experimental procedure section.

#### **4.2.2. Buffer Tests**

The control of pH and mixing of the chemical in the cores was a major concern. The preliminary ambient tests indicated that the use of a buffer solution could potentially solve this problem. As a result, the buffer (Borax) was utilized in several preliminary core

TABLE 4.2 The Effect of CO<sub>2</sub> Residual Saturation on Core Sample Permeability

<u>Original Permeability (md)</u>	<u>Permeability After CO<sub>2</sub> Flood (md)</u>	<u>Average % Reduction</u>
126	78	38
181	120	34
148	85	43
135	87	36

tests. Table 4.3 summarizes the results of the core tests with the buffer. The results indicate that the buffer has failed to maintain the pH in the core samples. It is believed that the Berea sandstone core adsorbed sufficient OH<sup>-</sup> ions to reduce the pH such that little or no precipitate was formed.

#### **4.2.3. Experimental Procedure**

The procedure employed for core tests involved six steps: core preparation, core mounting, permeability measurement, pre-test treatment, testing, and post-test treatment.

The core preparation procedure was performed prior to any testing with each core and is listed below:

1. Each core was numbered, measured, and placed in a drying oven for 48 hours.
2. The cores were then weighed and the weights were recorded.
3. The cores were sealed in a stainless steel core holder and evacuated for two hours.
4. The core holder was filled brine and pressurized to 100 psig for 24 hours to insure complete saturation of the cores.
5. The cores were removed from the core holder, weighed and the weights were recorded.
6. Porosity and pore volume of each core were calculated and recorded.
7. The cores were stored in brine under ambient conditions until needed for testing.

TABLE 4.3 Core Test Results Utilizing Buffer Solution at 1500 psig and 100°F

<u>Chemical</u>	<u>Pre-Test Permeability (md)</u>	<u>Post-Test Permeability (md)</u>	<u>% Reduction</u>
CaCl <sub>2</sub>	91	88	3
BaCl <sub>2</sub>	95	99	0

Note: Only a very slight amount of precipitate was noticed on the inflow face of the Calcium treated core and none was noticed on the Barium.

The next step, core mounting, was performed with each core before each individual test. Figure 4.1 is a schematic diagram of the core holder. The procedure for core mounting was as follows:

1. A 6-1/2 inch piece of shrink tubing was cut and placed over the core.
2. End caps with a section of stainless steel tubing were placed on the ends of the core inside the shrink tubing.
3. The tubing was shrunk onto the core and end caps using a heat gun.
4. The shrink tubing was trimmed and sealed to the end caps using epoxy on the ends.
5. The core was placed into the core holder by threading the inlet tubing through the closed end of the core holder after the epoxy hardened.
6. The cap was placed over the outlet tubing and tightened to seal the core inside the holder.
7. A fitting was attached on the closed end to seal the core holder and to contain the overburden pressure.

The third procedure in core testing was the permeability measurement. Figure 4.2 illustrates the experimental set-up for core tests. The procedure for permeability measurements is listed below:

1. The core holder was filled with water around the core and place in line.
2. Overburden pressure was adjusted at 250 psig using a mercury pump.

3. Brine was pumped through the core for 45 minutes at a flow rate of 400 ml/hr.
4. The outlet of the core was opened to ambient conditions (0 psig).
5. Once the pressure drop stabilized and was recorded, the brine flow rate was measured in cc/sec and recorded.
6. The beginning permeability was then calculated using Darcy's equation.

$$K = \frac{Q\mu L}{(P_1 - P_2)A}$$

K = permeability (darcies)

L = length of the core (cm)

Q = flow rate (cc/sec)

$\mu$  = viscosity of permeability test brine (cp)

A = area of core ( $\text{cm}^2$ )

$P_1 - P_2$  = pressure drop across the core (atm)

The next step was to perform a pre-test  $\text{CO}_2$  flooding to account for permeability reduction due to  $\text{CO}_2$  residual saturation in the core. The procedure for pre-test  $\text{CO}_2$  treatment is listed below:

1. The Isco precision pump was filled with brine.
2. 250 psig overburden pressure was put on the core.
3. The air was purged from the lines using the pump and a vent line at the entrance to the core.

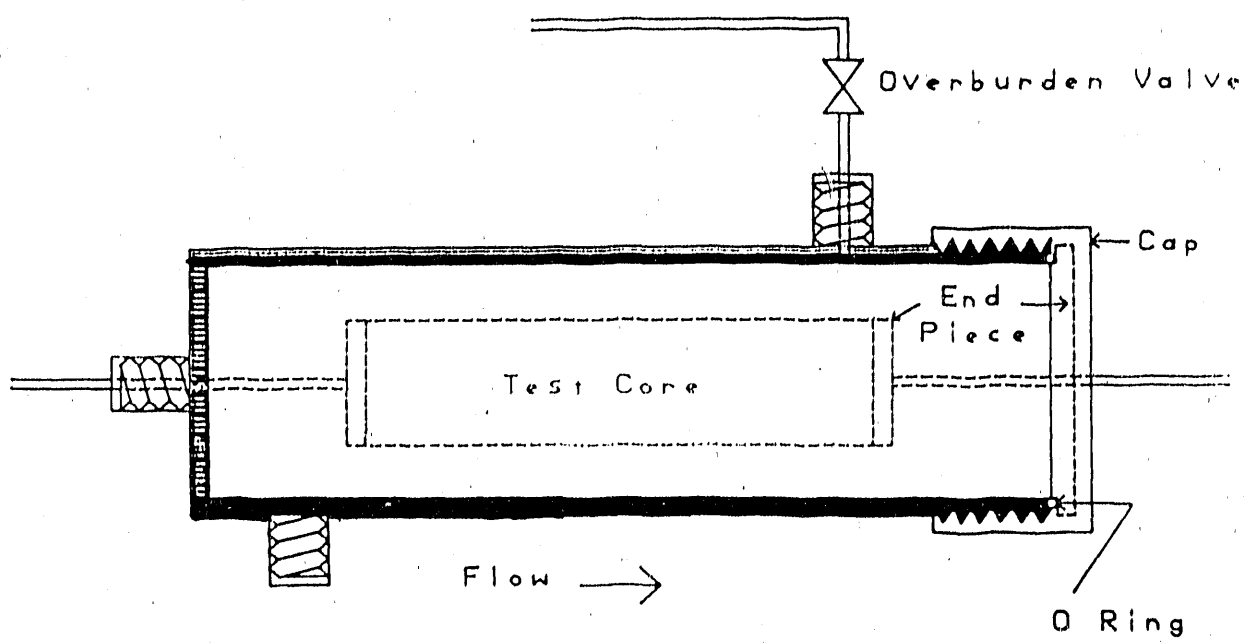


Fig. 4.1. The Schematic Diagram of the Core Holder

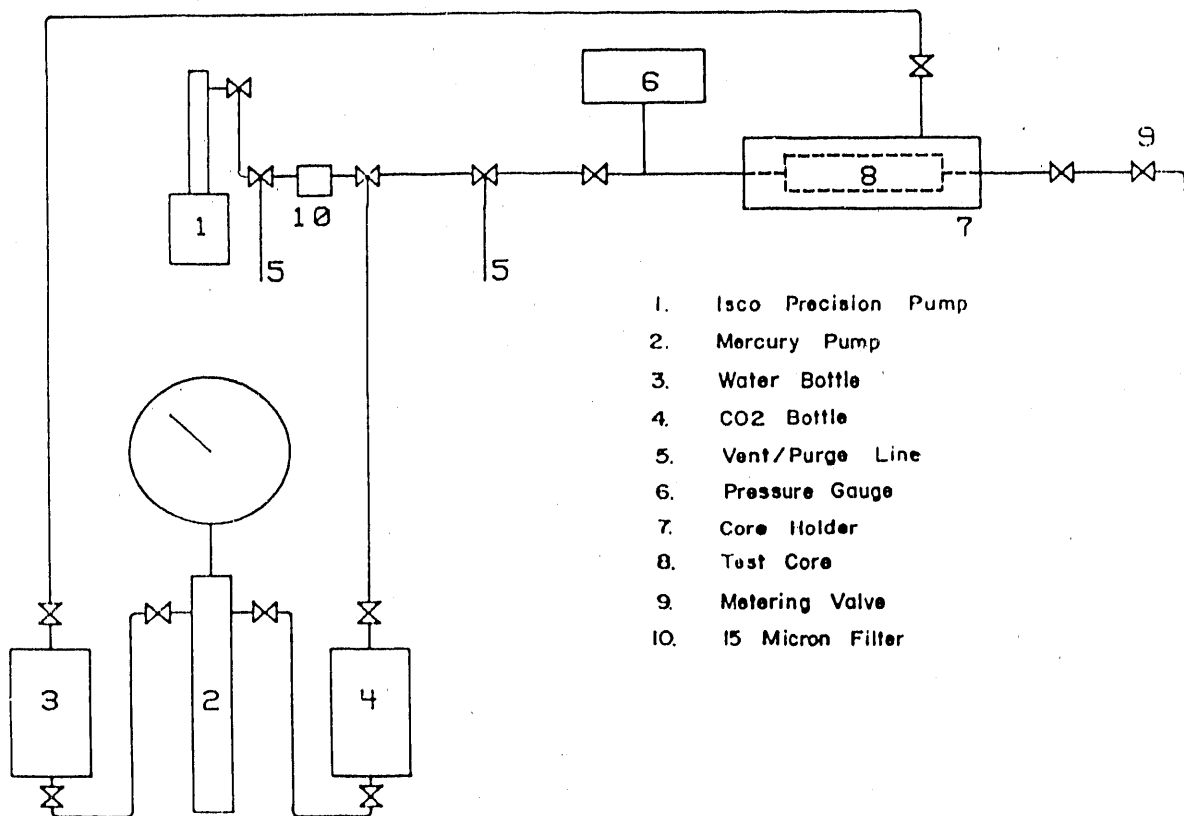


Fig. 4.2. The Schematic Diagram of the Experimental Set-up for Single Core Tests

4. The pressure transducer was adjusted to 0 psig.
5. The vent line valve was closed and the pump was turned on (downstream end of the core was opened to ambient pressure).
6. 2 PV (approx. 80 cc) of brine were pumped through the core at 400 ml/hr.
7. After 2 PV, the valve was closed at the downstream end of core.
8. Flow of brine was continued and pressure was raised to test pressure.

Note: While the pressure built, overburden pressure was maintained at 500 psi over the core pressure.

9. Upon reaching the planned pressure, flow was reduced to 67% of 400 ml/hr and the downstream valve was opened enough to allow flow while maintaining  $\pm 100$  psig of test pressure.
10. 2 PV of test solution was pumped through the core at test pressure and 67% of 400 ml/hr rate.
11. After 2 PV of flow, the core was shut in maintaining  $\pm 100$  psi of test pressure.
12. Overburden pressure was checked and shut in at 500 psi over the test pressure.
13. The mercury pump was converted over from overburden pressure to the CO<sub>2</sub> source by redirecting the appropriate valves on the mercury pump.
14. The line from the CO<sub>2</sub> bottle to the vent line just ahead of core was purged with CO<sub>2</sub> and reclosed.
15. The CO<sub>2</sub> pressure was raised to the test pressure.

16. The upstream valve of core was opened allowing CO<sub>2</sub> to enter the core.
17. Simultaneously, pumping and opening of the downstream valve was continued to flow CO<sub>2</sub> through the core.
18. 1 PV (approx. 35 cc) of CO<sub>2</sub> flowed through the core at  $\pm 100$  psi of the test pressure.
19. Upon completion of CO<sub>2</sub> flow, the core was closed in maintaining test pressure.
20. Step 13 was reversed, returning the controls of overburden pressure to the mercury pump.
21. The CO<sub>2</sub> line was then purged with brine from the pump.
22. Pressure in the line was returned to test pressure using brine.
23. The upstream valve of the core was opened, then the downstream valve was opened enough to allow 67% of 400 ml/hr flow rate and  $\pm 100$  psi of test pressure.
24. 2 PV of brine was pumped through.
25. After 2 PV of brine, the pump was shut off and allowed to slowly reach ambient pressure (overburden pressure was simultaneously lowered maintaining a +500 psi differential).
26. The pump was refilled with brine.
27. Overburden pressure was set at 250 psig.
28. The pump was turned on and the flow lines were purged.

29. The vent line was opened and the pressure transducer was rechecked (must read 0 psig).
30. The vent line was closed and the pump was set at 400 ml/hr.
31. Brine was pumped at 400 ml/hr.
32. When the brine flow reached the downstream port of the core (drips out end a timer was started).
33. Flow continued for 45 minutes.
34. After 45 minutes, a graduated cylinder was placed under the downstream port to catch the effluent.
35. A stop watch was started when the first drop entered the graduated cylinder and time was measured until 30 cc of effluent was collected.

Details of the precipitation test procedure are:

1. The core holder containing the core was placed in line and one pressure transducer was connected upstream of the core.
2. The pump line, downstream flow line, and overburden pressure line were connected to the core holder.
3. Required overburden pressure (250 psig) was maintained on the core by utilizing the mercury pump.
4. A heating jacket was placed on each core and the temperature was raised to the desired level.

5. The precision pump was charged with an adequate amount of the test chemical ( $\text{BaCl}_2$  or  $\text{CaCl}_2$ ) and 2 PV was pumped through the core at ambient pressure while the temperature was rising. Flow rate was 400 ml/hr.
6. During step 5, the temperature was monitored to ensure that the temperature had stabilized.
7. The flow of the test chemical was continued with the downstream valve closed allowing pressure to build up to reach desired test pressure. The pump flow rate was then reduced to 67% of 400 ml/hr.

Caution: Overburden pressure must remain 500 psi above that of the core, thereby preventing the shrink tubing around the core from expanding.

8. 2 additional PVs of the test chemical were pumped through the core by opening the downstream valve slightly so that the 67% of 400 ml/hr flow rate can be obtained.
9. At completion of the desired chemical volume, the upstream and downstream valves were closed isolating the core to maintain the test pressure.

Note: Overburden and core pressures were closely monitored. Differential heating, in some cases, caused pressure differences.

10. Flow was stopped, and the pressure was released by opening the proper vent line.

11. The CO<sub>2</sub> source was connected to the sample train.
12. The line from the CO<sub>2</sub> bottle to the vent line just ahead of the core was purged with CO<sub>2</sub> and reclosed.
13. The pressure in the CO<sub>2</sub> line was raised to or slightly above the core/test pressure.
14. The upstream valve was opened to allow CO<sub>2</sub> to enter the core. 35 cc of CO<sub>2</sub> (approx. 1 PV) were allowed to flow at desired pressure by opening the downstream valve. Pressure was maintained at  $\pm$ 100 psi of test pressure.
15. Upon completion of CO<sub>2</sub> flow, the upstream and downstream valves were closed to maintain pressure.
16. The CO<sub>2</sub> source was removed from the testing apparatus.
17. The pump was filled with an adequate volume of NaOH and the flow lines were purged.
18. The pressure of flow line was raised utilizing the pump and NaOH.
19. Upon reaching core/test pressure, the upstream valve was opened to allow NaOH to enter the core.
20. The downstream flow valve was opened and 2 PVs were pumped through the core maintaining the pressure to within  $\pm$ 100 psi of the test pressure. Flow rate was 67% of 400 ml/hr.

21. After completion of step 20, the core was shut in by closing upstream and downstream valves.
22. Step 10 was repeated.
23. The pump was filled with an adequate volume of brine and the flow lines were purged.
24. The line pressure was raised to the core/test pressure and the upstream valve was opened to allow brine to enter the core.
25. 2 PVs of brine were pumped, maintaining pressure at  $\pm 100$  psi of the desired test pressure at a flow rate of 67% of 400 ml/hr.
26. On completion of brine volume, flow was stopped and the upstream valve was closed, allowing core pressure to bleed down to ambient.

Note: Overburden pressure must be reduced gradually as core pressure decreases, maintaining 500 psi over the core pressure. When core pressure reached ambient, overburden was also lowered to ambient.

27. Heating jackets were shut off and removed. (This was done in conjunction with step 25 or 26.)
28. The pump was flushed to rinse out chemicals and all flow lines were purged.

The final stage of this procedure was the post-test stage described below:

1. After the overburden pressure was reduced to 0 psig, the core holder was removed from the line.

2. The core holder was drained and the core removed.
3. The shrink tubing was removed from the core and the core was placed in a weak hydrochloric acid solution to dissolve the precipitate from it. This procedure allowed the cores to be re-used.
4. The cores were left in this solution for approximately 48 hours and were then placed in a brine solution at ambient conditions until needed again.

#### **4.2.4. Single Core Test Results**

Table 4.4 summarizes the results of the single core precipitation experiments at 1500 psig and 100°F. The results for both  $\text{CaCl}_2$  and  $\text{BaCl}_2$  clearly indicate that precipitate forms in the core sample under dynamic conditions. A 40% reduction in permeability on the average was observed in the case of Calcium. For Barium, an average of only 21% reduction in permeability was observed. It should be mentioned that Barium produces more precipitate than Calcium under the same conditions; however,  $\text{BaCO}_3$  has a much smaller particle size, causing it to migrate through the core. As a result, the use of Barium salt would result in lower permeability reduction. Table 4.5 summarizes the results of the experiments at 2000 psig and 100°F. A similar permeability reduction has occurred in the Calcium case; that is, an average of 38 percent. The Barium, however, resulted in an average of a 31% reduction, which is higher than the 1500 psig tests.

TABLE 4.4 Single Core Tests Results at 1500 psig and 100 °F

<u>Chemical</u>	<u>Pre-test</u>	<u>Core Permeability (md)</u>	<u>% Reduction</u>
		<u>Post-test</u>	
CaCl <sub>2</sub>	115	77	38
CaCl <sub>2</sub>	98	62	39
CaCl <sub>2</sub>	95	49	48
CaCl <sub>2</sub>	83	41	51
CaCl <sub>2</sub>	70	53	24
BaCl <sub>2</sub>	80	72	10
BaCl <sub>2</sub>	38	32	16
BaCl <sub>2</sub>	116	78	33
BaCl <sub>2</sub>	116	86	26

TABLE 4.5 Single Core Tests Results at 2000 psig and 100°F

<u>Chemical</u>	<u>Pre-test</u>	<u>Core Permeability (md)</u>	<u>% Reduction</u>
		<u>Post-test</u>	
CaCl <sub>2</sub>	84	53	37
CaCl <sub>2</sub>	49	30	39
BaCl <sub>2</sub>	70	46	34
BaCl <sub>2</sub>	43	31	28

#### **4.2.5. Aging Tests**

After the chemical precipitation was completed, it was decided that a series of aging tests would be carried out. These tests lead to the knowledge of the stability of the in situ chemical precipitates. This was done by measuring the permeability of the core after a period of 1, 3, and 5 days, respectively. Table 4.6 provides the aging tests results at 1500 psig and 100°F. For Calcium precipitate, the permeability increased only slightly after a duration of 5 days. On the other hand, permeability in the case of the Barium precipitate appears to be increasing with time more significantly than the Calcium precipitate case. This can be explained by the difference in the particle size between the two carbonate precipitates. The Calcium carbonate, forming larger particles, would most likely stay in the pore spaces (plugged passageways) during the flooding. When the brine flows through the core, Barium Carbonate, on the other hand, which has a smaller particle size, would probably migrate down stream and would not be retained in the core.

#### **4.3. Multiple Core Tests**

To improve the sweep efficiency during CO<sub>2</sub> flooding, it is desirable to reduce the permeability of the larger pores throughout the flood pattern. Therefore, the depth of the propagation of carbonate precipitation is another topic of concern. The objective of this series of tests was to determine whether

TABLE 4.6 Aging Test Results at 1500 psig and 100°F

<u>Chemical</u>	<u>Pre-test</u>	<u>Core Permeability (md)</u>	<u>Core Permeability (md)</u>		
		<u>Post-test</u>	<u>Day 1</u>	<u>Day 2</u>	<u>Day 3</u>
CaCl <sub>2</sub>	98	62	65	59	76
CaCl <sub>2</sub>	95	49	57	57	62
CaCl <sub>2</sub>	83	41	44	49	52
BaCl <sub>2</sub>	38	32	37	43	46
BaCl <sub>2</sub>	116	78	80	84	91
BaCl <sub>2</sub>	116	86	100	100	100

the precipitate can alter the permeability some distance away from the point of injection. To achieve the objective, a series of tests were conducted, utilizing 2 (or 3) 6-inch cores connected together. Cores with similar permeabilities were connected one after the other with an additional transducer set between each core holder. Figure 4.3 illustrates the experimental set-up for the two-core tests. The experimental procedure was similar to the single core experiments; however, the volume of chemicals were doubled (or tripled, in the case of 3-core tests). The permeability reduction was evaluated for each core.

The results in Table 4.7 indicate that the precipitation process can be extended away from the injection point as evidenced by permeability reduction in the second and third cores. In the case of Calcium Carbonate, for the 2-core test, the front core had more permeability reduction than the rear core. It was possible, that after the injected  $\text{CO}_2$  reacted with the chemicals in the front core, less mixing would occur in the second core; thus, less precipitate would be formed. In the Barium Carbonate tests, a reverse behavior was observed. More permeability reduction was observed in the rear core than the front core. This was most likely caused by the smaller Barium Carbonate particles migrating downstream, causing a larger permeability reduction in the second core. The results of the 3-core tests also indicate that the permeability in all the cores in the set was reduced. The reduction in the permeability was more in the first core (closest to the injection point) than in the second core. However, a large reduction in permeability was observed in the final core. This can be attributed to an additional pressure drop in the

final core. The reduction in pressure allowed some CO<sub>2</sub> to be released from the solution, thereby, increasing the pH of the solution, which in turn, promotes additional carbonate precipitation. The permeability reduction in the final core is, therefore, sensitive to the magnitude of the pressure drop and pH requirement for precipitate formation.

#### **4.4. Relative Permeability Tests**

The previous tests have clearly indicated that carbonate precipitate forms under flowing conditions in the core samples. In addition, the results indicated that carbonate precipitate plugs the pores, thereby, reducing the permeability of the core. It is, however, desirable to know if the pore plugging has preferentially occurred in the larger and more permeable pores. This objective can be achieved by comparing liquid-gas relative permeabilities before and after carbonate precipitation. It should be noted that, generally, the high mobility gas tends to flow through the larger pores while the liquid tends to flow through smaller pores. Consequently, a reduction in gas relative permeability after the precipitation would indicate that the majority of the precipitate has been formed in the larger pores as previously envisioned.

##### **4.4.1. Relative Permeability Test Apparatus**

The relative permeabilities were evaluated utilizing a gas-water relative permeability apparatus. The gas-water relative permeability apparatus is designed to permit the

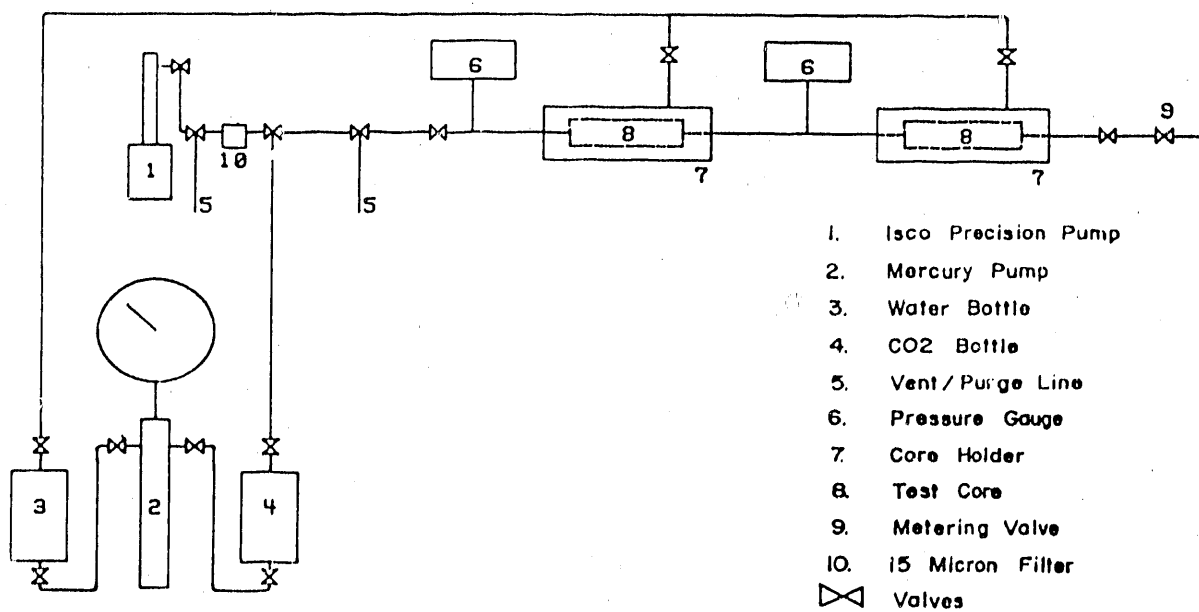


Fig. 4.3. The Schematic Diagram of the Experimental Set-up for Multiple Core Tests

TABLE 4.7 Multiple Core Tests Results at 1500 psig and 100°F

<u>Chemical</u>	<u>Core Position</u>	<u>Core Permeability (md)</u>		<u>% Reduction</u>
		<u>Pre-test</u>	<u>Post-test</u>	
$\text{CaCl}_2$	Upstream	63	48	24
	Downstream	85	74	13
$\text{CaCl}_2$	Upstream	60	49	18
	Middle	46	41	11
	Downstream	58	22	62
$\text{BaCl}_2$	Upstream	66	43	35
	Downstream	49	28	43
$\text{BaCl}_2$	Upstream	44	37	23
	Middle	47	40	15
	Downstream	42	20	52

simultaneous measurements of gas and water flow rates for a sample subjected to an external gas-drive under a constant pressure differential. A schematic diagram of the laboratory equipment used to perform gas-water relative permeability tests is shown in Figure 4.4. The apparatus consists of a pressure control panel, a Hassler core holder panel, and a glassware volumetric measuring system panel<sup>(1,2,3)</sup>.

The pressure control panel consists of three pressure regulators and gauges, a multi-valve system and a gas humidifier cylinder. The compressed air source, which was used for the displacement gas, is connected to the pressure control panel and is flowed through the gas humidifier cylinder to the regulators. Thus, by the use of the three regulators any desired working pressure range from 0 - 400 psi may be accurately maintained<sup>(1,2,3)</sup>.

The gas is then flowed to the Hassler core holder panel. The core holder pressure (overburden pressure) is obtained from a nitrogen source connected directly to and gauged by the core holder panel. Attached to the outlet end of the core holder is the water collection burette. The displacement gas is flowed through the core holder, through the collection burette, into the volumetric measuring system panel<sup>(1,2,3)</sup>.

The volumetric measuring system consists of a burette and three calibrated bottles. The amount of gas flowed into the volumetric panel is measure by the amount of water that is displaced from the previously filled burette and calibrated bottles. If the water level in the largest of the three calibrated bottles reaches the mark indicating a

total produced volume of 1750 cc's, flow is then diverted to a wet test meter which can be attached to the volumetric measuring system panel<sup>(1,2,3)</sup>.

#### **4.4.2. Relative Permeability Test Procedure**

The core samples used to perform the gas water relative permeability tests had diameters of 1-1/2 inches to accommodate the core holder. The core holder used was designed to handle samples varying in length from 1.5 to 5.5 cm. The core samples were cut to lengths approaching the maximum length of the core holder to reduce "end-effects". After the air permeabilities and porosities had been determined, the cores were placed in a pressure vessel and saturated with the desired brine solution for approximately 48 hours to insure complete saturation. Each core sample was weighed before and after saturation. The dry and saturated weights, along with the measured density of the saturant, was used to calculate pore volume with that measured previously on the dried sample for conformation that the sample was completely saturated.

It must be noted that, due to the unknown amount of chemical precipitation, a dry weight could not be obtained for the test cores after the chemical precipitation experiment was conducted. Therefore, the above saturation check would not be performed on the precipitated cores. However, since it was performed on the cores before precipitation when establishing the reference clean core permeabilities, and if the results were in agreement that complete saturation was obtained it was assumed that

the saturation process was correct in obtaining complete saturation.

Note: Refer to the Schematic diagram of the gas-water relative permeability test apparatus in Fig. 4.4 to identify the valves and flow lines being referenced.

1. The three calibrated bottles and components, burette of the volumetric measuring system were filled with distilled water and all valves were set as instructed in the core laboratories operations manual.
2. The saturated cores were loaded into the Hassler core holder.
3. The receiving tube and stopper were assembled.
4. The delivery tube was inserted into the prepared hole in the stopper. The stopper was moved up on the delivery tube until the end of the delivery tube was below the wide diameter portion of the receiving tube.
5. The rubber stopper attached to the glass tube connected to line B, was inserted into the open end of the burette of the volumetric measuring system.
6. Line B was connected to the brass hose connection which is part of the receiving tube assembly.
7. Making sure valves 6 and 7 are closed, the displacement gas source was turned on and, by use of the pressure panel, the pressure was regulated until the desired differential pressure was obtained.
8. Valve 13 was opened, moving the water level in the burette slightly to the right. This was caused by a slight increase in the gas volume in the receiving tube

and in connecting line B. This was due to a small reduction in pressure resulting from the bead of water in the burette. If there are no leaks in the system, the water level can be positioned so that after opening valve 13, the right hand side of the water level will shift exactly to the "start" marker. If, however, the water level comes to rest either to the right or the left of this mark, (right-hand) edge of the water level, as indicated by the burette calibrations, it should be noted. This incremental volume should then be added, if the leading edge is to the left of "start", or subtracted if to the right, to each of the preselected levels of total fluid production when recording these data for subsequent calculation purposes.

9. The test was started by simultaneously opening valve 6 and starting the timer. As the leading edge of the water level reached each of the preselected calibration marks, the water production (cc), time (sec) and gas injection pressure (psi), are read simultaneously. Each set of readings were recorded on the data sheet opposite the total volume reading (corrected if necessary) corresponding to the calibration mark.
10. When the water level in the largest of the three calibrated bottles reached the mark indicating a total produced volume of 1750 cc's, rotate the handle of valve 9 was rotated through 90 degrees of arc in a clockwise direction while simultaneously closing valve 8. Measurements of the total produced volume were continued with the wet-test meter.

11. When the test was complete, valve 12 was opened to drain any water that might have collected in the trap. This was prior to cutting off the injected gas.
12. The core sample was then unloaded.

#### **4.4.3. Relative Permeability Data Analysis**

This section describes the method used to determine the relative permeabilities from the experimental results.

Recording the cumulative total volume of gas and water,  $V_n$  (cc), at the out-flow end of the sample, at atmospheric pressure, during the experiment, enables the calculation of the incremental produced gas and water volume,  $V_i$  (cc), at atmospheric pressure.

$$V_i = V_n - V_{n-1} \quad (4.2)$$

Likewise, recording the cumulative total volume of water,  $W_n$  (cc), in the same manner and conditions as that of the gas and water,  $V_n$ , enables the calculation of the incremental produced water,  $W_i$  (cc), at atmospheric pressure.

$$W_i = W_n - W_{n-1} \quad (4.3)$$

The incremental volume of gas,  $dG_i$  (cc), produced at the out-flow end of the sample at atmospheric pressure ( $cm^3$ ) is then computed as:

$$dG_i = V_i - W_i \quad (4.4)$$

The average produced gas water ratio,  $R_i$  (cc/cc), at atmospheric pressure for any

given production interval is found by:

$$R_i = dG_i/dW_i \quad (4.5)$$

By taking the differential flooding pressure,  $dP$  (psia), the Boyles Law correction factor for mean pressure,  $C_1$ , is:

$$C_1 = 14.7/(14.7 + dP/2) \quad (4.6)$$

The average flowing gas-water ratio,  $R_f$  (cc/cc), in the core sample at mean pressure conditions for any given production interval is:

$$R_f = R_i \times C_1 \quad (4.7)$$

Using the viscosity ratio,  $\mu_g/\mu_w$  (cp/cp), the gas-water relative permeability ratio,  $K_{rg}/K_{rw}$ , is:

$$K_{rg}/K_{rw} = ((V_i - W_i)/W_i)(C_1)(\mu_g/\mu_w) \quad (4.8)$$

The Log-Mean average of the gas and water flow increment for any given production interval,  $(V_i)_{l.m.}$  (cc), measured at atmospheric, is essentially equivalent to a geometric average of a logarithmic plot. The log-mean between log 1.00 and log 2.0 is log 1.414; hence:

$$(V_i)_{l.m.} = 0.414(V_i) \quad (4.9)$$

The average total volume of gas and water,  $(V_i)_{avg}$  (cc), produced through any given production interval, measured at atmospheric conditions may be found by taking the total cumulative gas and water produced through the preceding step and adding the log-mean average gas produced for the current step:

$$(V_i)_{avg} = (V_i)_{n-1} + (V_i)_{l.m.} \quad (4.10)$$

The arithmetic average of water produced through any given production interval,  $(dW_i)_{avg}$  (cc), is equivalent to the geometric average for a linear plot, and is expressed:

$$(dW_i)_{avg} = 0.500(W_i) \quad (4.11)$$

The average total volume of water,  $(W_i)_{avg}$  (cc), produced through any given production step:

$$(W_i)_{avg} = (W_i)_{n-1} + (dW_i)_{avg} \quad (4.12)$$

The average total volume of gas produced at out-flow end,  $G_i$  (cc), through any given production step, referred to atmospheric conditions is:

$$G_i = (V_i)_{avg} - (W_i)_{avg} \quad (4.13)$$

The average total volume of gas,  $G$  (cc), and the average total volume of gas and water,  $V$  (cc), produced through any production step, referred to mean pressure conditions, is:

$$G = G_i(C_i) \quad (4.14)$$

$$V = G + (W_i)_{avg} \quad (4.15)$$

The ratio of total water and gas flow at mean pressure to the water flow,  $1/f_w$  (cc/cc), is:

$$1/f_w = R_i + 1.00 \quad (4.16)$$

The saturation increment between the average gas saturation and the terminal gas saturation,  $dS$ , obtained near the out-flow face of the core sample, is:

$$dS = f_w(G + (W_i)_{avg}) = f_w(V) = V/(1/f_w) \quad (4.17)$$

Thus, the calculation of the end face gas saturation,  $V_g$ , is:

$$V_g = (W_i)_{avg} - f_w(V) = (W_i)_{avg} - dS \quad (4.18)$$

When expressed as a fraction of pore volume, the terminal or end-face gas saturation,  $S_g$  (cc/cc), is:

$$S_g = V_g/P.V. \quad (4.19)$$

A flow constant,  $C_2$  (sec/cc), must then be computed by the equation:

$$C_2 = (\mu_g)(L)(14.7)(10)(C_1)/(A)(K)(dP) \quad (4.20)$$

where:  $L$  = total length of sand, cm

$\mu_g$  = viscosity of displacing phase, cp

$A$  = cross-sectional area of sample,  $cm^2$

$dP$  = pressure drop across sample, psia

$K$  = permeability, md

The gas flow rate,  $Q_g$  (cc/sec), is:

$$Q_g = dG_g/dT \quad (4.21)$$

where,  $dT$  is the incremental time of any given production step (seconds).

The relative permeability to gas  $K_{rg}$ , the fraction of air permeability at 100% gas saturation, is:

$$K_{rg} = Q_g(C_2) \quad (4.22)$$

The average gas saturation  $Sg_2$ , fraction of P.V., is:

$$Sg_2 = (W_i)_{avg} - P.V. \quad (4.23)$$

Once this point has been reached in the calculation procedure, the values found may be plotted and, through graphical interpretation, a corresponding relative permeability to water  $K_{rw}$ , for each of the cores may be obtained. The relative permeability ratios are plotted versus the endface displacing phase gas saturations on semi-log paper. The relative permeabilities to the displacing phase,  $K_{rg}$ , are plotted versus the average displacing phase saturations on coordinate paper. Relative permeability ratios and relative permeabilities to the displacing phase can then be picked from their respective plots at a common displacing phase saturation. Relative permeabilities to water are then calculated by dividing the relative permeability to the displacing phase by the relative permeability ratio at the same saturation<sup>(1,2,3,4,5,6,7)</sup>.

By following the calculation procedures described here, the calculations may be set up in tabular/spreadsheet form. A spreadsheet was constructed, using LOTUS 123, to perform the calculations required before graphical techniques were applied. Constants used in the calculations were stored in the spreadsheet, thereby, requiring only the entering of the test results to execute the spreadsheet. Once the results from the spreadsheet were obtained, they were plotted to determine  $K_w$  graphically.

#### 4.4.4. Relative Permeability Test Results

To establish a valid reference, the core relative permeability ratio for clean core tests (Cores A and B) was compared to published data<sup>(3)</sup> as illustrated in Figure 4.5. The

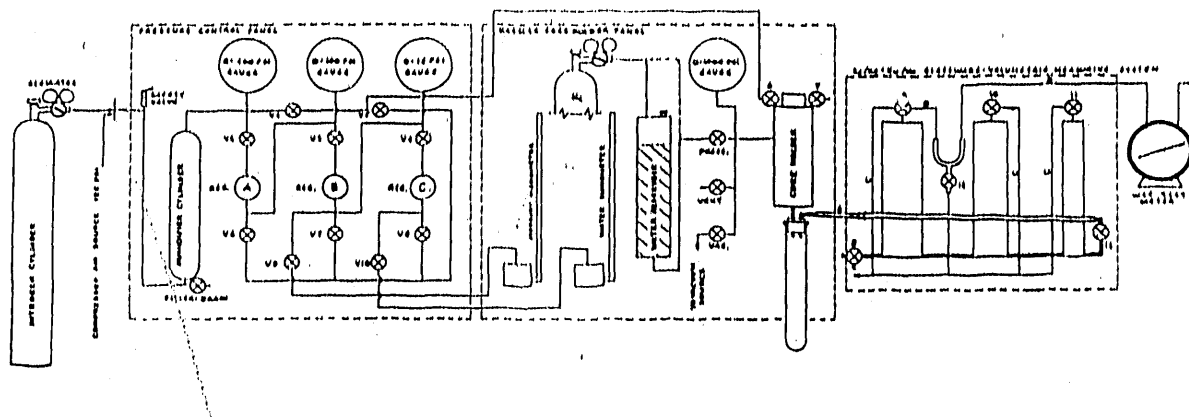


Fig. 4.4 The Schematic Diagram of Gas-Water Relative Permeability Test Apparatus <sup>(1)</sup>

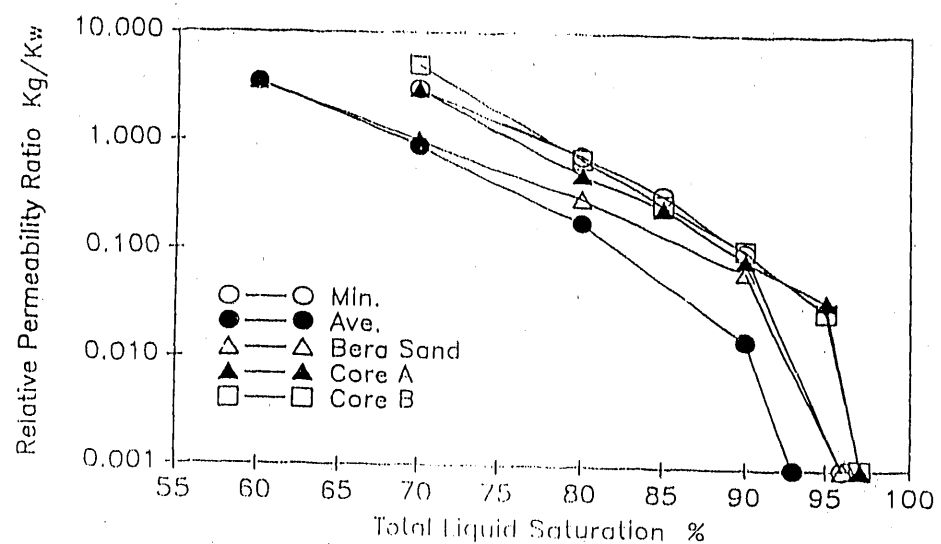


Fig. 4.5. The Comparison of Measured Relative Permeability Ratios with Published Data <sup>(3)</sup>

results indicate that the measured relative permeabilities are within the generally established values than validating the experimental procedures and results. Figures 4.6 through 4.9 illustrate the measured core original relative permeabilities and altered relative permeabilities due to  $\text{CaCO}_3$  and  $\text{BaCO}_3$  precipitation under different test conditions.

The comparison of pre- and post-precipitation relative permeabilities indicates that the relative permeabilities to gas have declined after precipitation while liquid permeability has increased. The observed reduction in gas relative permeability can be attributed to the formation of precipitate selectively in the high permeability zones since the gas flows more readily in the larger and more permeable pores. This indicates that the permeability profile has been modified as anticipated. The results also indicate that Calcium Carbonate reduces the relative permeability to gas more than Barium Carbonate. The pressure of 1500 psig seems to provide the best results for Calcium while 2000 psig provides better results for Barium.

#### **4.5. Multiple Slug - Multiple Core Test**

To gain additional insight into the permeability profile modification, a multiple slug test was conducted in 3 cores with approximately the same permeability connected in series. These groups of tests were conducted by injecting 3 slugs of salt solution ( $\text{CaCl}_2$  or  $\text{BaCl}_2$ ), each followed by a slug of

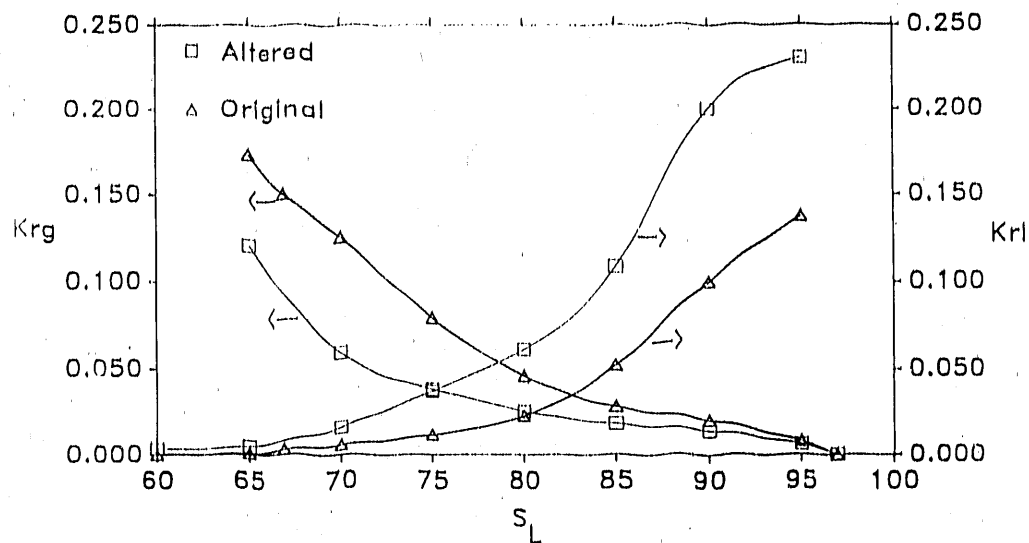


Fig. 4.6. The Effect of Calcium Carbonate Precipitation at 1500 psig and 100°F on the Relative Permeability of the Berea Core Sample

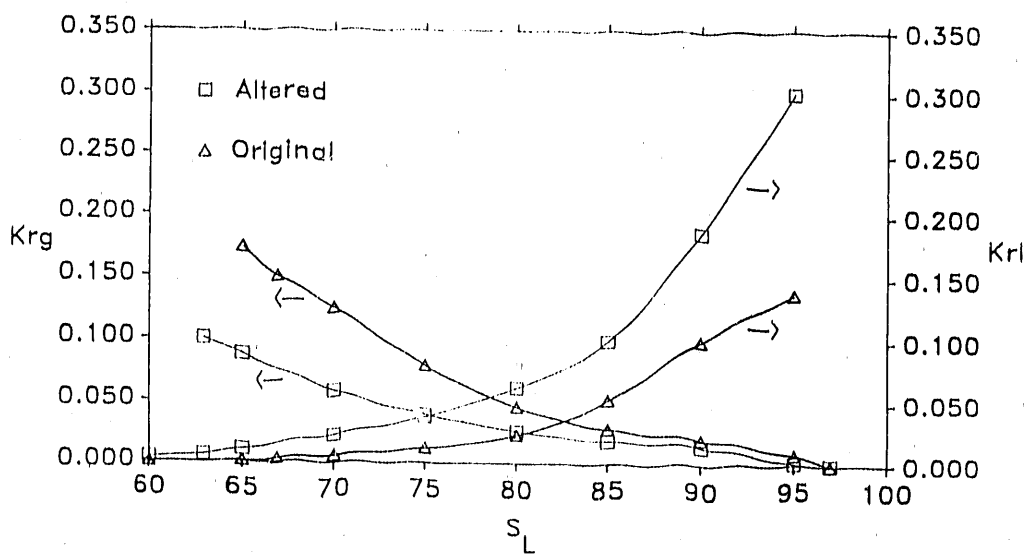


Fig. 4.7. The Effect of Calcium Carbonate Precipitation at 2000 psig and 100°F on the Relative Permeability of the Berea Core Sample

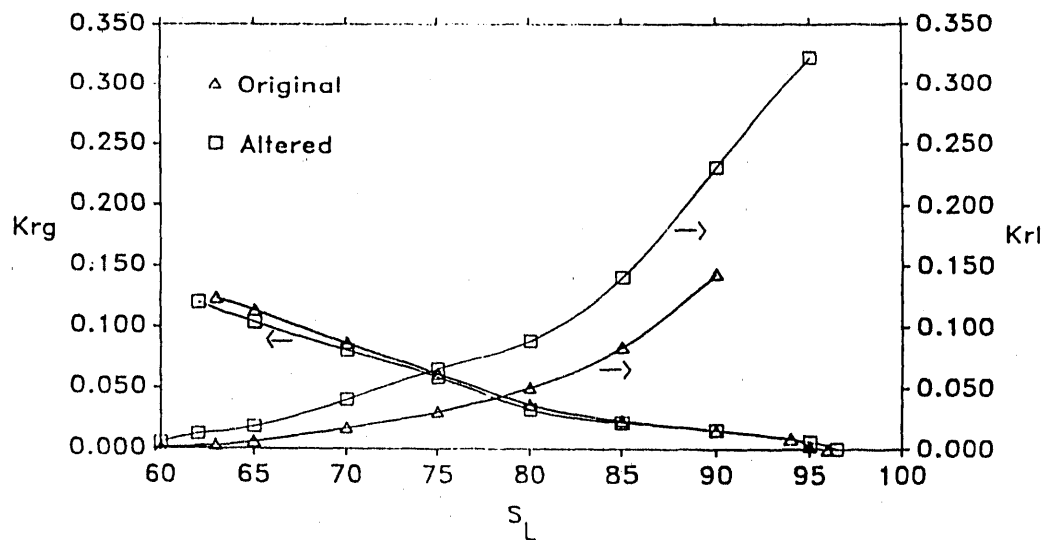


Fig. 4.8. The Effect of Barium Carbonate Precipitation at 1500 psig and 100°F on the Relative Permeability of the Berea Core Sample

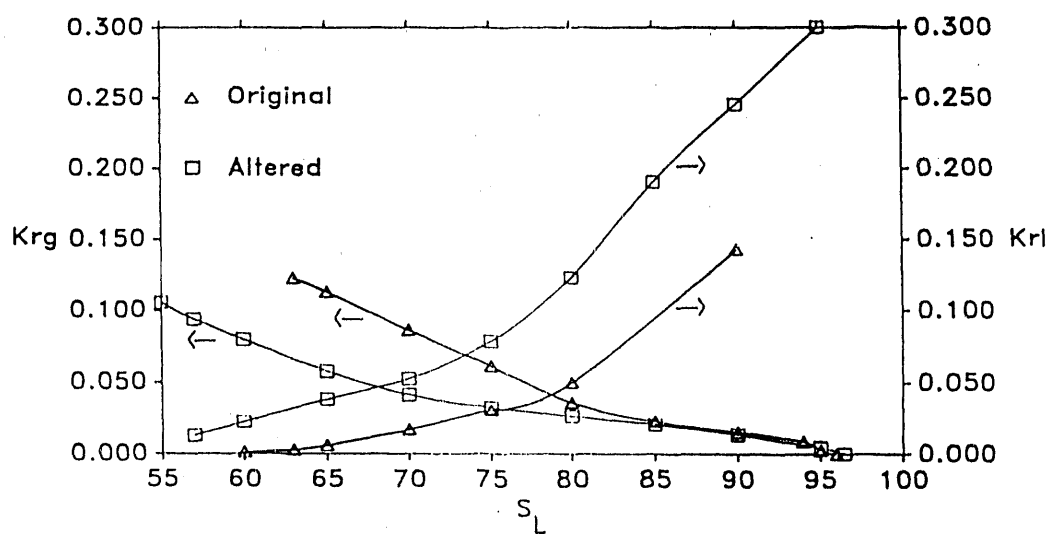


Fig. 4.9. The Effect of Barium Carbonate Precipitation at 200 psig and 100°F on the Relative Permeability of the Berea Core Sample

$\text{CO}_2$  and  $\text{NaOH}$ . After each set of slugs, the cores were flushed with brine and the permeability and relative permeability of the core samples were measured. The results of permeability reductions are given in Table 4.10. The gas relative permeability reductions are shown in Figures 4.10 and 4.11. Figure 4.10 represents the typical behavior of the 3 core samples for  $\text{CaCO}_3$  precipitate and the first 2 core samples for  $\text{BaCO}_3$  precipitation. Figure 4.11 illustrates the gas relative permeability reduction in the final core sample (the 3rd core) for  $\text{BaCO}_3$  precipitation.

The results in Table 4.8 indicate that precipitation reduces the permeability of the core samples after each slug. It can also be concluded that the reduction in permeability can be extended away from the injection point. However, the reduction in relative permeability after the second slug is not significant except for the last core during the  $\text{BaCO}_3$  precipitation. It is believed that the pressure reduction in the 3rd core resulted in additional  $\text{BaCO}_3$  precipitation. The reduction in pressure allows some  $\text{CO}_2$  to be released from the solution, thereby, increasing the pH of the solution. The higher pH promotes  $\text{BaCO}_3$  precipitation. It should be noted that the same is true for the 3rd core in the  $\text{CaCO}_3$  precipitation test. However,  $\text{CaCO}_3$  requires a higher pH than  $\text{BaCO}_3$  to precipitate which was not achieved by pressure reduction during the test. This however does not mean that  $\text{CaCO}_3$  precipitation does not occur in the field due to pressure reduction near the production well.

#### **4.6. Oil Saturated Core Tests**

A series of tests were designed to study the additional oil recovery by CO<sub>2</sub> due to carbonate precipitation. These experiments were performed in core samples saturated with oil. Three procedures for saturating the Berea sandstone cores with crude oil were tested in order to determine the most efficient method of core saturation. The first method started with the cores dry. The cores were numbered, weighed, and measured, and the data were recorded. The dry cores were then mounted in stainless steel core holders in the same manner as in the core tests. The crude oil was then pumped into the core at 250 psig for two hours. Approximately ten pore volumes of oil was pumped through each core. The "saturated" cores were then weighed and stored in a container filled with the same crude.

The second method used the same procedure except for the condition of the cores prior to flowing the oil. In these tests, the cores were saturated with brine before they were mounted in the core holders. When saturated with the oil, the oil displaced the brine. Again, the oil was pumped at 250 psig until no brine was visible in the effluent. Again, it was approximately ten pore volumes.

The third saturation procedure was done by numbering, weighing, and measuring dry cores. The cores were then placed dry in a large stainless steel core holder and sealed in. The core holder was then placed under vacuum for four hours. The vessel was then filled with the crude oil and, when the negative pressure stabilized, a slight

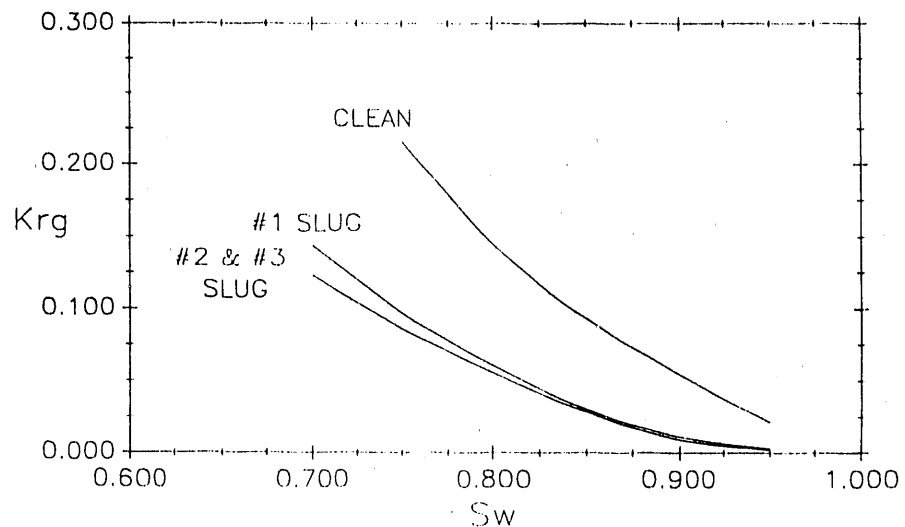


Fig. 4.10. The Effect of Carbonate Precipitation on Gas Relative Permeability in Multi-Slug Tests

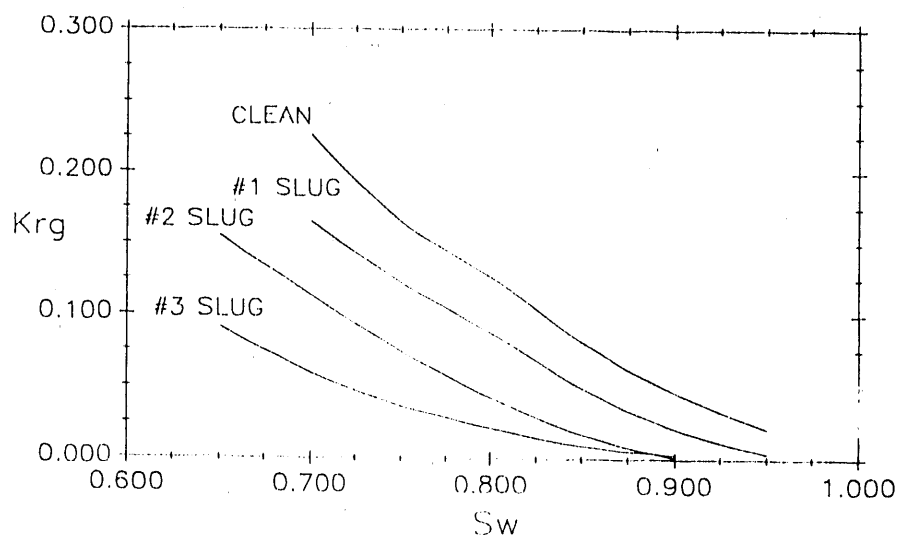


Fig. 4.11. The Effect of Barium Carbonate Precipitation on the 3<sup>rd</sup> core in the Multi-Slug Tests

**TABLE 4.8 Permeability Reductions During the Multiple Slug Experiment  
in 3 Connected Cores at 1500 psig and 100°F**

<u>Salt</u>	<u>Core #</u>	<u>Slug #</u>	<u>% Reduction</u>
CaCl <sub>2</sub>	1	1	30
	1	2	21
	1	3	25
CaCl <sub>2</sub>	2	1	32
	2	2	40
	2	3	28
CaCl <sub>2</sub>	3	1	40
	3	2	45
	3	3	7
BaCl <sub>2</sub>	1	1	45
	1	2	22
	1	3	8
BaCl <sub>2</sub>	2	1	30
	2	2	32
	2	3	19
BaCl <sub>2</sub>	3	1	53
	3	2	47
	3	3	28

positive pressure (approximately 50 psig) was applied. The cores then remained in the holder under pressure for 48 hours.

In all three procedures, the cores were wiped off and weighed after the saturation process was completed. Also, all the cores were placed in a container filled with the crude oil for storage. Results reveal that the most complete saturation occurred in the third procedure utilizing the vacuum.

The experimental procedures for the oil saturated core tests are described below:

1. The oil saturated core was placed in test apparatus and flooded with oil to insure saturation.
2. The core was water flooded with brine, all effluent was collected until no additional oil could be flushed from the core. The volume of the oil displaced was measured.
3. The core was then flooded with  $\text{CO}_2$ , again the effluent was collected and the oil displaced was measured.
4. The precipitation test was performed on core. All effluent was collected in order to measure any oil that was flushed out as the precipitate began.
5. The  $\text{CO}_2$  flood was repeated and all effluent was collected and the oil displaced was measured.

All oil collected after step three of the procedure can be attributed to the permeability reduction due to the carbonate precipitation. The results from the tests did yield a 30% to 35% recovery of the residual oil. The cores have an approximate pore

volume of 35cc. The initial water and CO<sub>2</sub> flood provided the recovery of an additional 4 to 5 cc of the residual oil with the second CO<sub>2</sub> flood. However, these results revealed that experiments of this nature could not be reliably performed within the scope of this project due to the scale of the experimental apparatus. The experimental design of the process replicates both a water flood and a CO<sub>2</sub> flood. Because of the size of the cores, the water flood and the CO<sub>2</sub> pumped through the core prior to the precipitation formation process recovered nearly all of the saturated oil, leaving an insignificant residual oil level.

#### **4.7. Discussion**

The experimental results clearly indicate that the carbonate precipitation treatment has the potential to modify the permeability profile to provide better CO<sub>2</sub> mobility control. However, there are a number of questions that need to be answered before the treatment can be considered for field applications. The major problem is achieving the necessary pH to form precipitate. During laboratory experiments, NaOH was utilized to achieve a pH of about 8. However, controlling the pH in the flood pattern could be significantly more difficult. The pH of the reservoir brine can play a significant role. If the reservoir pH is low (3-4), the pH control is more difficult. The reaction of NaOH with the reservoir rock can further complicate the problem. However, if the pH is higher (6-7) the problem will be much less. Unfortunately, the lower pH range is more representative of the reservoir pH. In addition, the mixing of two liquid phases (i.e. CaCl<sub>2</sub> and NaOH) is

necessary to obtain the precipitate. Establishing a moving mixing zone in the porous media can also influence the results of the treatment in the field.

#### **4.8. Summary and Conclusions**

The results of the experimental research studies indicated that:

1. Carbonate precipitate can be formed under flowing conditions in the core samples.
2. The precipitate selectively reduces the permeability of the larger pores by reduction of gas relative permeability in favor of liquid permeability.
3. The precipitation can be propagated in the porous media to modify the permeability profile throughout the flood pattern.
4. The carbonate precipitation has the potential to provide better  $\text{CO}_2$  mobility control.
5. The pH requirements for precipitation formation can complicate field application of this treatment.

#### 4.9. References

1. "Core Laboratories Relative Permeability Test Manual", Core Laboratories, Inc., Dallas, TX, Catalog No. 103.
2. Morse, R.A., Terwilligere, P.L. and Yuster, S.T.: "Relative Permeability Measurements on Small Core Samples", Oil Gas J., 23:109-125, 1947.
3. Osoba, J.S., Richardson, J.G. and Blair, P.M.: "Laboratory Measurements of Relative Permeability", Trans. AIME, 192:47-56, 1951.
4. Jones, S.C. and Roszelle, W.O.: "Graphical Techniques for Determining Relative Permeability from Displacement Experiments", J. Pet. Technol., pp. 807-817, May 1978.
5. Owens, W.W., Parrish, D.R. and Lamoreaux, W.E.: "An Evaluation of a Gas Drive Method for Determining Relative Permeability Relationships", Trans. AIME, 207:275-280, 1956.
6. Johnson, E.F., Bossler, D.P. and Naumann, V.O.: "Calculation of Relative Permeability from Displacement Experiments", Trans. AIME, 216:370-372, 1959.
7. Amyx, J.W., Bass, D.M., Jr., Whiting, R.L.: "Petroleum Reservoir Engineering", McGraw Hill Book Company, Inc., New York, 1960.

## CHAPTER FIVE

### **SIMULATION STUDIES**

#### **5.1. Introduction**

The purpose of this phase of the research was to extend the experimental results to field applications through computer simulation, and to determine the enhancement in the horizontal and vertical sweep efficiencies due to carbonate precipitation. The experimental results have clearly indicated that the carbonate precipitation has the potential to modify the permeability profile. A reservoir model was utilized during this phase of research to illustrate the effects of permeability profile modification on oil recovery by  $\text{CO}_2$  flooding.

It should also be noted that pH requirements for carbonate precipitation can limit the depth of permeability profile modification during the field application. In the laboratory experiments  $\text{NaOH}$  was utilized to achieve a pH of about 8 in the core samples. The pH control in the reservoir is, however, significantly more complicated. In addition, the mixing of two liquid phases (i.e.,  $\text{CaCl}_2$  and  $\text{NaOH}$ ) is necessary to form the precipitate. Establishing a moving mixing zone in the porous media can also limit the depth of permeability profile modification. Therefore, simulation studies were also conducted to investigate the effect of the depth of permeability modification on  $\text{CO}_2$  sweep efficiency enhancement.

## 5.2. Description of the Reservoir Model

The performance of the heterogeneous reservoirs cannot be predicted by "classical" reservoir engineering tools which are based on homogeneous prototypes. To predict the performance of the heterogeneous reservoirs, it is necessary to describe the reservoir heterogeneity. The numerical reservoir models (simulators) utilize the fundamental equations for fluid flow in porous media and also account for many variations in the reservoir rock and fluids properties. These variations are accounted for by dividing the reservoir into many blocks or grids and assigning a different set of properties to each grid-block. The reservoir simulators provide a numerical solution for the system of equations that is resulted from applying the fundamental flow equation to each grid-block. Over the past two decades. Increasingly sophisticated numerical models for simulating fluid flow in complex reservoirs has been developed. Today, reservoir simulation has become an essential part of reservoir engineering studies.

To determine the sweep efficiency enhancement by carbonate precipitation during miscible WAG  $\text{CO}_2$  displacement, MASTER, an extended black-oil reservoir simulator was employed. This section provides only a brief description of MASTER. The complete description of the simulator and its capabilities can be reviewed elsewhere<sup>(1,2)</sup>.

MASTER is referred to as an extended black-oil simulator since it takes the concept of solubility (solution gas to oil) and formation volume factor from black oil simulators and extends them to multiple soluble species. The modifications for the multi-

component simulator is the same as conventional models with an additional data set describing the stock tank oil-solvent interactions. MASTER is an extension of the black oil simulator BOAST (Black Oil Applied Simulation Tool) developed by Fanchi, et.al.<sup>(3)</sup>. MASTER is similar to the Todd, et.al.<sup>(4)</sup> multicomponent simulator in that it uses mixing parameters, and programmed switching between the miscible and immiscible phases.

Many modifications to BOAST were necessary to account for the miscible process. Some of these were: 1) the addition of a fourth conservation equation to enable the tracking of oil, gas, water, and a solvent, 2) the addition of a mixing parameter developed by Todd and Longstaff<sup>(5)</sup> and later modified by Watkins<sup>(6)</sup>, and 3) reformulation of the solution method to a implicit pressure explicit saturation (IMPES) solution to account for gas injection. MASTER uses an iterative IMPES solution. First, the pressure equation is solved by estimating the pressure-dependent terms in the equation. Once the pressure is calculated, the pressure-dependent terms are estimated again, then are placed back into the pressure equation and solved again. This process is repeated until some convergence criterion is satisfied. MASTER also allows: 1) property weighing for upstream and average fluids, 2) the use of ten relative permeability/capillary pressure tables, 3) solvent loss to the aqueous phase, and swelling of oil from solvent solubility. It also allows the user to choose which relative permeability/capillary pressure tables to use, oil/gas, oil/water, or modified Stone's equation which uses both tables with a mixing parameter developed by Rosenzweig, et.al.<sup>(7)</sup> Miscibility in compositional simulators is

achieved by mixing the aqueous phase with the solvent and creating one flowing phase, this is not possible in a four species simulator. Therefore, MASTER uses the Chase and Todd<sup>(5)</sup> method to emulate miscibility.

### **5.3. Simulation Studies**

This section summarizes the results of preliminary cases that were considered for simulation. The permeability modification by carbonate precipitation was accounted for in the model by altering the permeability and relative permeability for a specific number of blocks prior to  $\text{CC}_2$  injection. The extent of permeability reduction was based on the laboratory results. Several relative permeability tables were also set up based on the results of the relative permeability measurements and were included in the model input data set. The post-precipitation relative permeability data set was assigned to the blocks where the permeability was altered to account for carbonate precipitation. Three cases were considered during this phase of study and the following sections provide the description and results for each case.

#### **5.3.1. Case 1: Immiscible Recovery Enhancement**

The first case simulated an immiscible  $\text{CO}_2$  WAG operation. A simple one-dimensional (line-drive) homogeneous reservoir consisting of 15 blocks as shown in Figure 5.1 was utilized for this case. Although this description is extremely simple and

does not represent actual reservoir situations, it can provide some insight into the effect of precipitation on oil recovery. The reservoir was first water flooded down to a water cut of 50% followed by an immiscible CO<sub>2</sub> WAG operations. The effect of precipitation was modeled by altering the permeability and relative permeability of a specific number of blocks prior to CO<sub>2</sub> injection.

Figure 5.2 summarizes the results in terms of dimensionless variables for the simulation runs performed during this case. It should be noted that, in this case, the relative permeability alteration is the main reason for the increase in oil recovery. Figure 5.2 illustrates that additional oil recovery as a result of the relative permeability alterations would be significant only when the relative permeability in at least 3 blocks (20% of reservoir) is altered. Beyond this point, significant (over 10%) additional recovery is achieved.

### **5.3.2. Case 2: Horizontal Sweep Efficiency Enhancement**

The second case simulated a miscible CO<sub>2</sub> WAG operation. A two-dimensional reservoir description as shown in Figure 5.3 (quarter of five-spot) was utilized. To illustrate the effect of heterogeneity on the oil recovery by CO<sub>2</sub> WAG operations, it was assumed that a zone with a higher permeability exists directly between the injection and production wells (the shaded area in Figure 5.3).

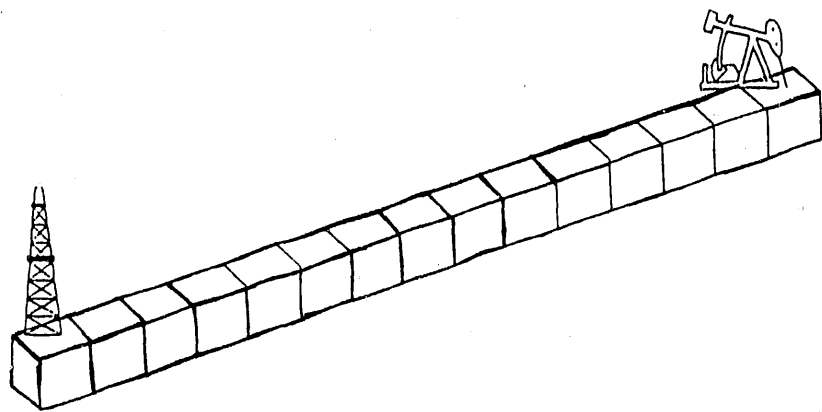


Fig. 5.1. The reservoir Model Used for Immiscible CO<sub>2</sub> Flooding Simulations

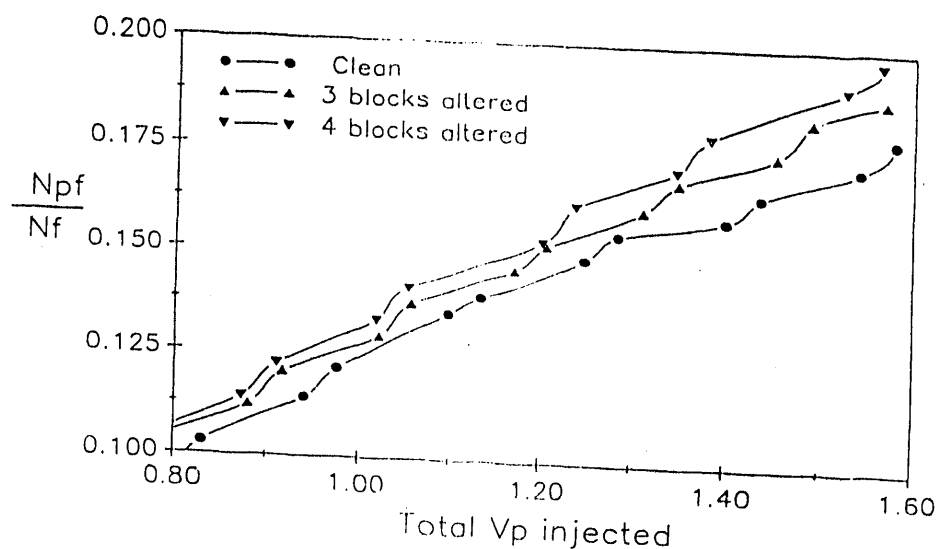


Fig. 5.2. The Effect of Precipitation on Oil Recovery Efficiency for Immiscible CO<sub>2</sub> Flooding

In this case, the reservoir was water flooded down to a water cut of 80% to reduce the oil saturation in most of the reservoir down to residual oil saturation. A CO<sub>2</sub> WAG was then initiated. Figure 5.4 compares the oil recovery for the heterogeneous reservoir as described above and a homogeneous reservoir with uniform permeability, equal to the overall average permeability of the heterogeneous case. As can be seen, the existence of the high permeability zone significantly reduces the areal sweep efficiency as evidenced by lower oil recovery. The effect of precipitation was modeled by altering the permeability and relative permeability of a specific number of blocks in the high permeability zone. Figure 5.4 also illustrates the oil recovery if the entire high permeability zone (11 blocks) was altered by precipitation. Although such a case is unlikely to occur in the field, it provides the upper limit or the potential for recovery enhancement through in-situ precipitation. Figure 5.5 illustrates the effective number of blocks that are altered in the high permeability zone on oil recovery. Again, it is necessary to alter at least 3 blocks (i.e. 27% of the zone) before significant improvements in oil recovery will be observed. Figures 5.6 and 5.7 compare the oil production rates for the various cases. Figures 5.8 and 5.9 illustrate the effect of the percentage of permeability reduction in the high permeability zone due to precipitation on oil recovery.

### **5.3.3. Case 3: Vertical Sweep Efficiency Enhancement**

The third case also simulated a miscible CO<sub>2</sub> WAG operation. A two-dimensional reservoir description as shown in Figure 5.10 (line-drive) was utilized. To illustrate the effect of permeability heterogeneity on oil recovery by CO<sub>2</sub> WAG operations, it was assumed that a streak of high permeability exists directly between the injection and production wells (shaded area in Fig. 5.10).

The reservoir was first flooded with water (to a water cut of 80%) in order to reduce the oil saturation in most of the reservoir to residual oil saturation. A CO<sub>2</sub> WAG was then initiated. Figure 5.11 compares the oil recovery for the heterogeneous reservoir as described above and a homogeneous reservoir with the permeability equal to the average value of the heterogeneous permeability case. As evidenced by lower oil recovery, the existence of the high permeability streaks significantly reduce the vertical sweep efficiency.

The effect of carbonate precipitation was then modeled by altering the permeability and relative permeability of a certain number of blocks in the high permeability streak by 40 percent. Figure 5.11 also illustrates the oil recovery if the entire high permeability streak was altered. Although such a case is unlikely to occur in the field, it provides the upper limit or the potential for recovery enhancement through in-situ precipitation. Figure 5.12 illustrates the results of scoping studies. As can be seen, to achieve improvements in vertical sweep efficiency, as few as 3 blocks need to be altered.

## Quarter Five Spot

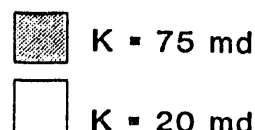
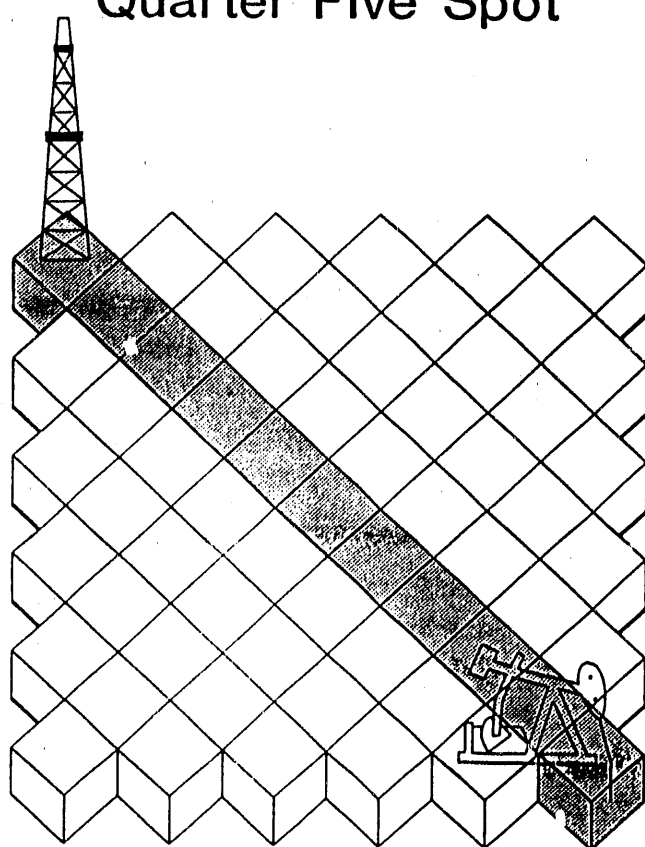


Fig. 5.3. The Reservoir Model Used for Horizontal Sweep Enhancement Simulations

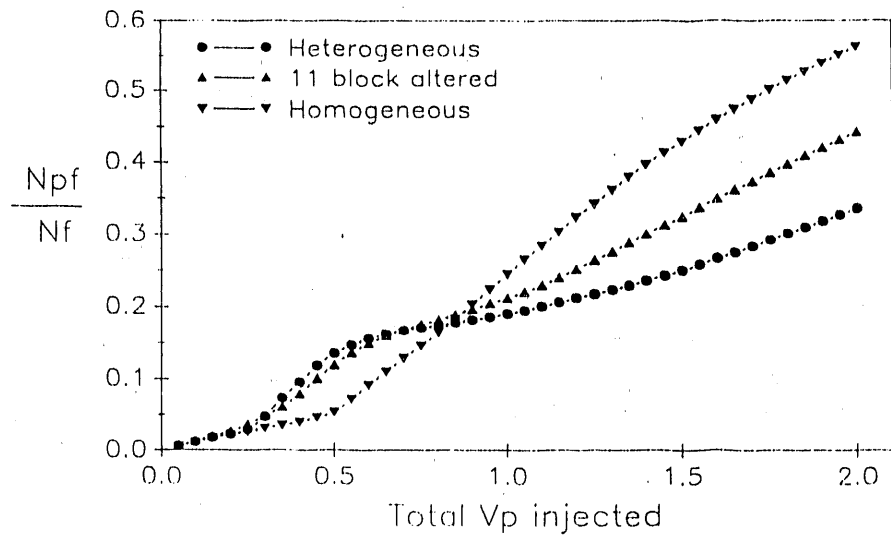


Fig. 5.4. The Effect of Horizontal Heterogeneity on Oil Sweep Efficiency by Miscible  $\text{CO}_2$  Flooding

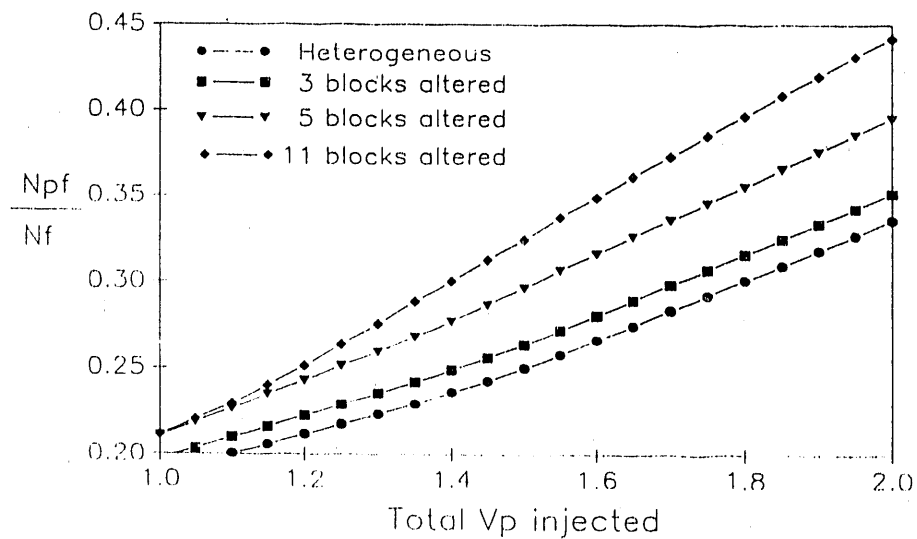


Fig. 5.5. The Effect of Precipitation Propagation on the Oil Horizontal Sweep Efficiency by Miscible  $\text{CO}_2$  Flooding

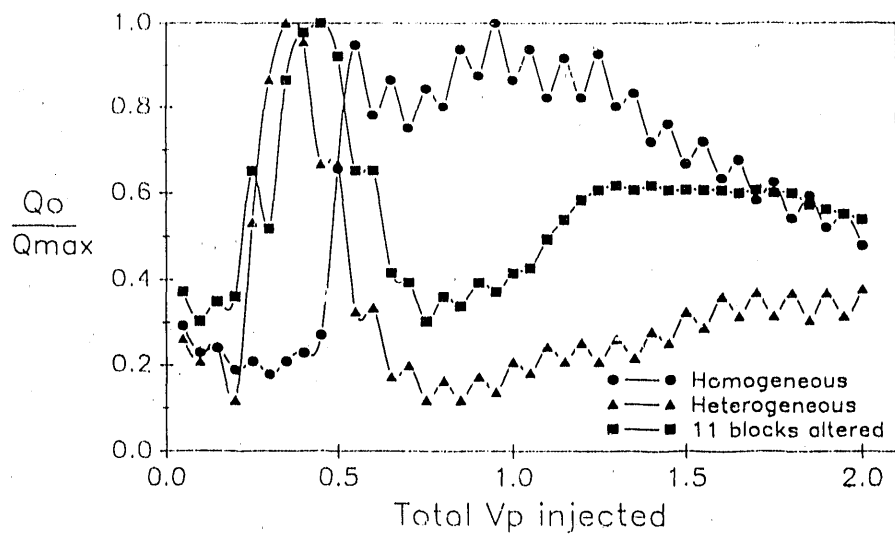


Fig. 5.6. The Effect of Horizontal Heterogeneity on Oil Production Rates During  $\text{CO}_2$  Miscible Flooding

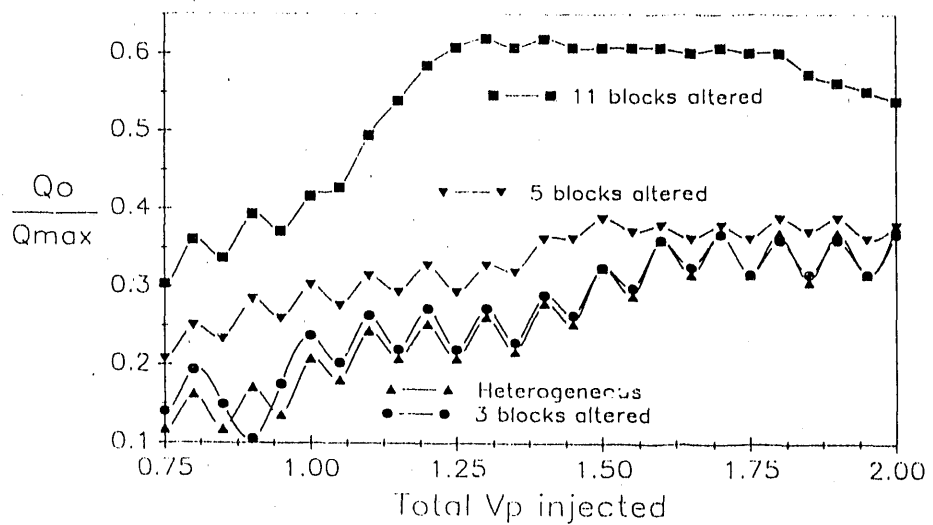


Fig. 5.7. The Effect of Precipitation Propagation on the Oil Production Rates During  $\text{CO}_2$  Miscible Flooding

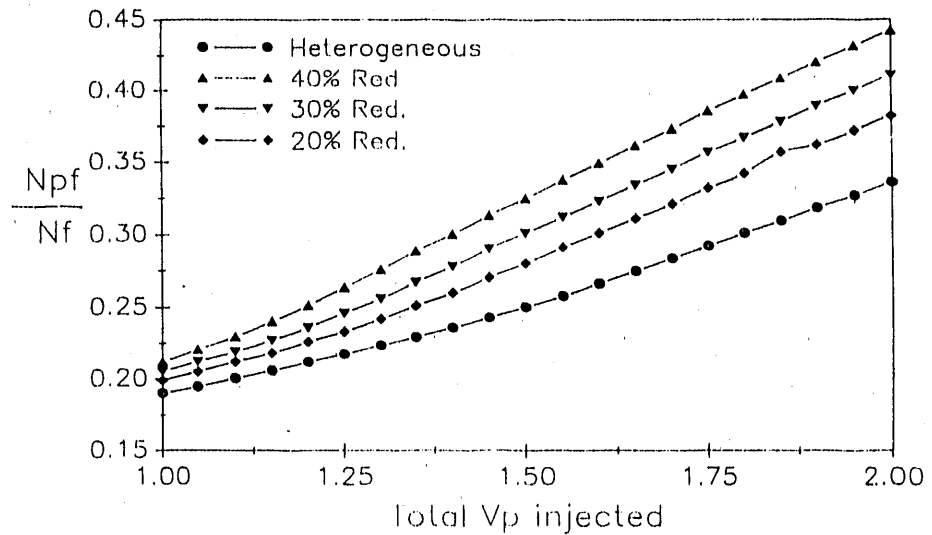


Fig. 5.8. The Effect of Percent of Permeability Reduction by Precipitation on Oil Sweep Efficiency

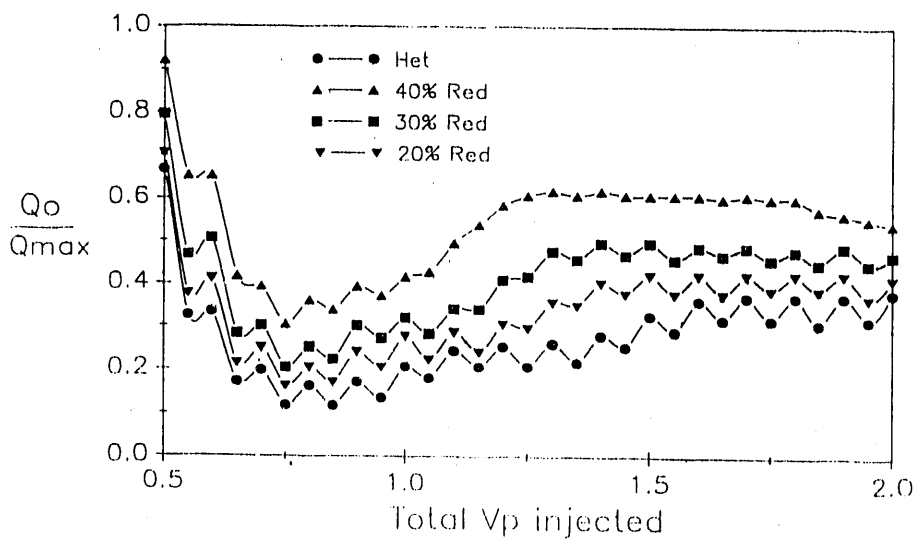


Fig. 5.9. The Effect of Percent of Permeability Reduction by Precipitation on Oil Production Rates

Figures 5.13 and 5.14 compare the oil production rates for the various cases.

#### **5.4. Summary and Conclusions**

The results of the computer simulation studies indicate that CO<sub>2</sub> vertical and horizontal sweep efficiencies can be enhanced by permeability profile modification. The scoping studies revealed that only a fraction of the high permeability zones (20% to 30%) need to be altered to achieve sweep efficiency enhancement. This is important since pH control in the reservoir limits the extent of permeability profile modification.

## DIRECT LINE DRIVE

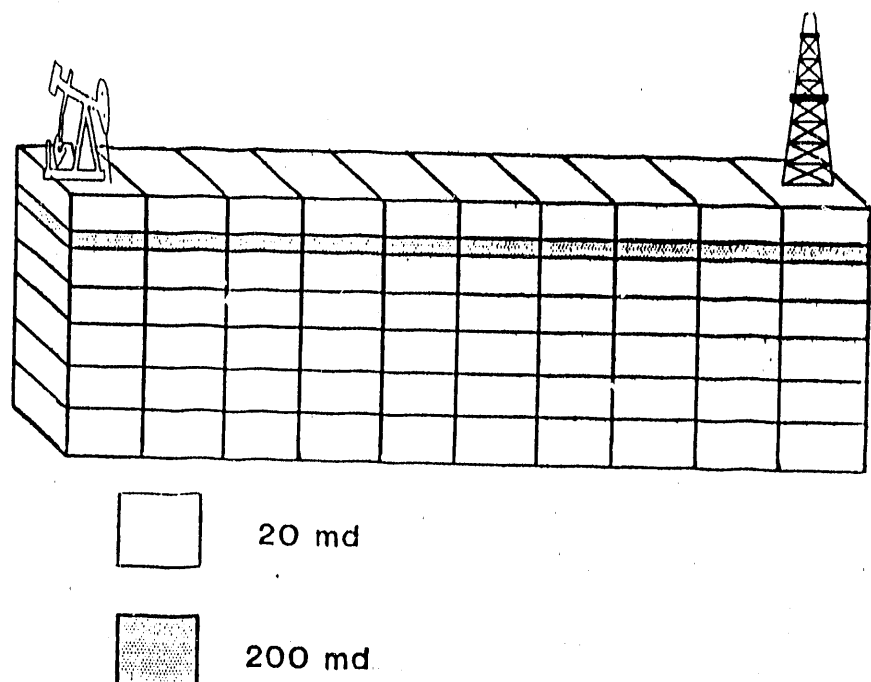


Fig. 5.10. The Reservoir Model Used for Vertical Sweep Efficiency Enhancement Simulations

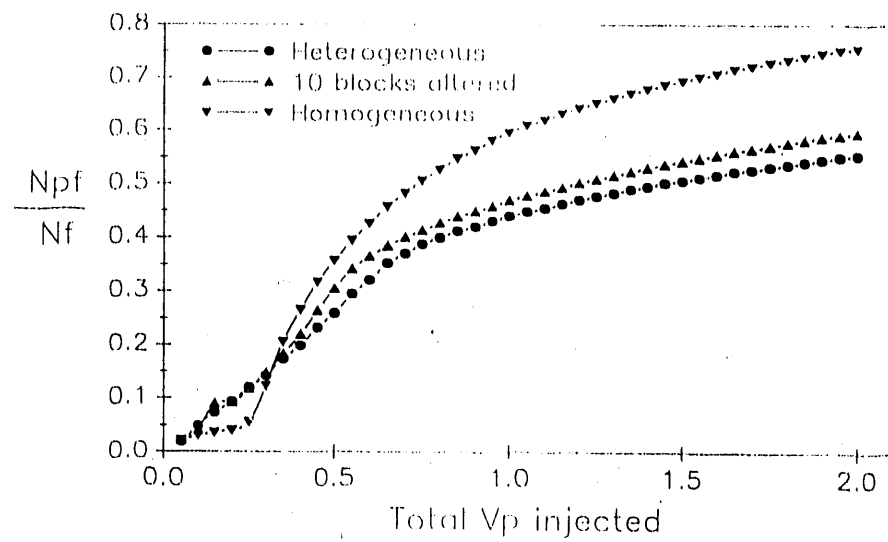


Fig. 5.11. The Effect of Vertical Heterogeneity on Oil Sweep Efficiency During Miscible  $\text{CO}_2$  Flooding

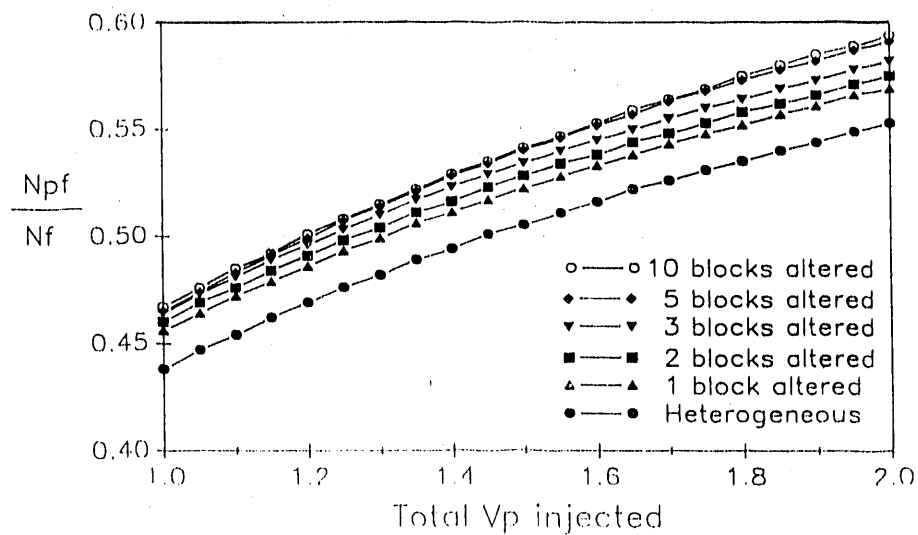


Fig. 5.12. The Effect of Precipitation Propagation on Oil Vertical Sweep Efficiency by Miscible  $\text{CO}_2$  Flooding

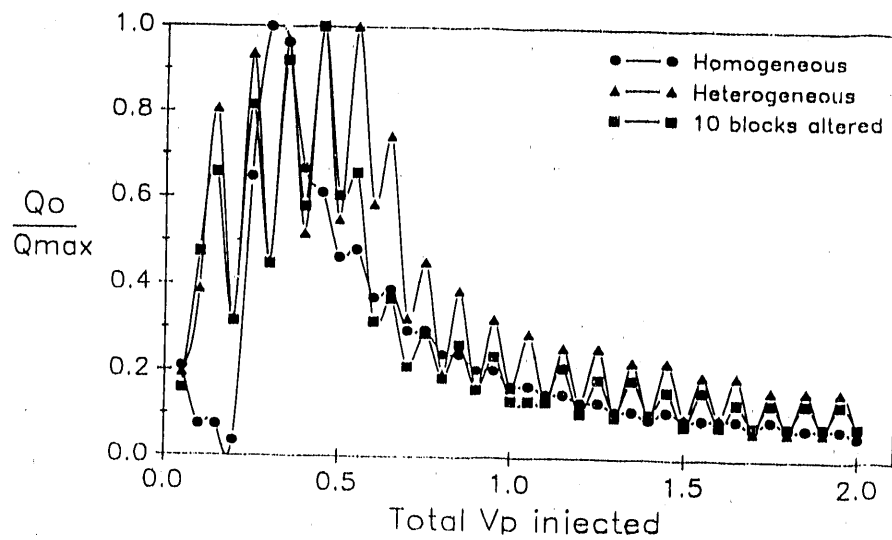


Fig. 5.13. The Effect of Vertical Heterogeneity on Oil Production Rates During  $\text{CO}_2$  Miscible Flooding

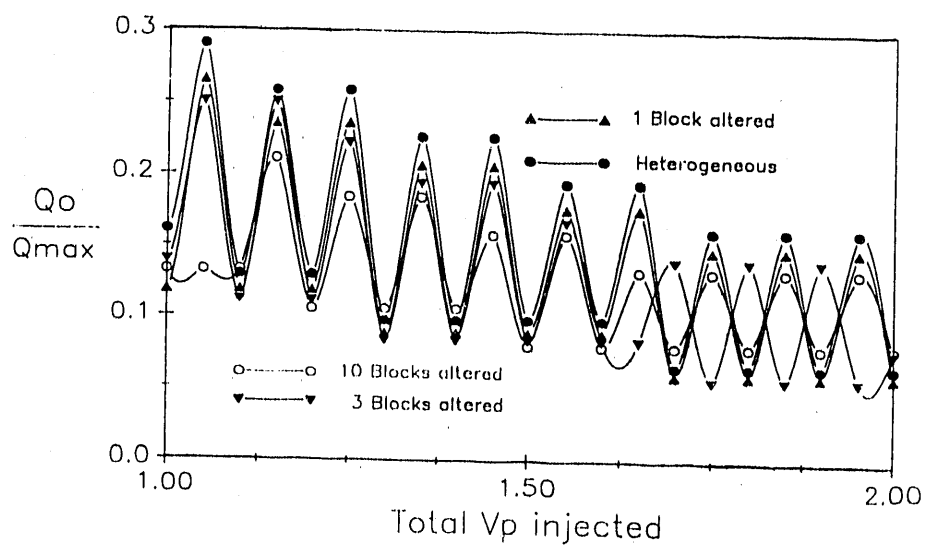


Fig. 5.14. The Effect of Precipitation Propagation on Oil Production Rates During  $\text{CO}_2$  Miscible Flooding

## 5.5. References

1. Lewin and Associates, Inc.: "User Guide and Documentation Manual for Miscible Applied Simulation Techniques for Energy Recovery", Report to DOE, 1985.
2. Ammer, J.R., Sams, W.N., and Brummert, A.C.: "An Extended Black Oil Simulator the Rigorously Treats Variable Bubble Point Problem", SPE 18533, Proc. of SPE Eastern Regional Conference, Charleston, WV, Nov. 1988.
3. Fanchi, J.R., Harpole, K.J., and Bujnowski, S.W.: BOAST: A Three-Dimensional Three-Phase Black Oil Applied Simulation Tool, User Manual, DOE/BC/10033-3, Sept. 1982.
4. Chase, C.A., Jr., and Todd, M.R.: "Numerical Simulation of CO<sub>2</sub> Flood Performance", Soc. Pet. Eng. Jour., Dec. 1984.
5. Todd, M.R. and Longstaff, W.J.: "The Development, Testing, and Application of Numerical Simulator for Predicting Miscible Flood Performance", Jour. Pet. Tech., July 1972.
6. Watkin, R.W.: "The Development and Testing of Sequential Semi-Implicit Reservoir Simulation Techniques", Soc. Pet. Eng. Jour., June 1972.
7. Rosenzweig, J.J., Abdalmalek, N.A., and Gochnour, J.R.: "The Development of Pseudo Functions for Three Phase Black Oil Simulators", Reservoir Characterization, L.W. Lake and H.B. Carroll, Jr. (eds.), Academic Press, Inc., 1986.

## NOMENCLATURE

A - area

$C_1$  - correction factor for pressure

$C_2$  - flow constant

$f_w$  - fractional flow of water

G - cumulative gas volume produced

K - permeability

$K_g$  - relative permeability to gas

$K_l$  - relative permeability to liquid

$K_w$  - relative permeability to water

L - length

$N_{pf}$  - cumulative oil production during  $\text{CO}_2$  flooding

p - pressure

$Q_g$  - gas flow rate

$Q_{max}$  - maximum oil production during  $\text{CO}_2$  flooding

$Q_o$  - oil production rate during  $\text{CO}_2$  flooding

$R_i$  - average produced gas-water ratio

$R_f$  - average flowing gas-water ratio

$S_g$  - gas saturation

$S_l$  - liquid saturation

$S_w$  - water saturation

V - total volume produced

$V_i$  - incremental volume produced

$V_p$  - reservoir pore volume  
 $W_i$  - incremental water produced  
 $\mu_g$  - gas viscosity  
 $\mu_w$  - water viscosity

# END

## DATE FILMED

07 / 18 / 91

